NAVAL POSTGRADUATE SCHOOL
Monterey, California

THESIS

HIGH EFFICIENCY SOLAR CELLS:
A MODEL IN SILVACO

by

Darin J. McCloy

September 1999

Thesis Advisor: Sherif Michael

Approved for public release; distribution is unlimited.

19991129 015

REPORT DOCUMENTATION PAGE

Form Approved
OMB No. 0704-0188

Public reporting burden for this collection of information is estimated to average 1 hour per response, including the time for reviewing instruction, searching existing data sources, gathering and maintaining the data needed, and completing and reviewing the collection of information. Send comments regarding this burden estimate or any other aspect of this collection of information, including suggestions for reducing this burden, to Washington headquarters Services, Directorate for Information Operations and Reports, 1215 Jefferson Davis Highway, Suite 1204, Arlington, VA 22202-4302, and to the Office of Management and Budget, Paperwork Reduction Project (0704-0188) Washington DC 20503.

1. AGENCY USE ONLY *(Leave blank)*	2. REPORT DATE	3. REPORT TYPE AND DATES COVERED
	September 1999	Master's Thesis

4. TITLE AND SUBTITLE
HIGH EFFICIENCY SOLAR CELLS: A MODEL IN SILVACO

5. FUNDING NUMBERS

6. AUTHOR(S)
McCloy, Darin J.

7. PERFORMING ORGANIZATION NAME(S) AND ADDRESS(ES)
Naval Postgraduate School
Monterey, CA 93943-5000

8. PERFORMING ORGANIZATION REPORT NUMBER

9. SPONSORING / MONITORING AGENCY NAME(S) AND ADDRESS(ES)

10. SPONSORING / MONITORING AGENCY REPORT NUMBER

11. SUPPLEMENTARY NOTES
The views expressed in this thesis are those of the author and do not reflect the official policy or position of the Department of Defense or the U.S. Government.

12a. DISTRIBUTION / AVAILABILITY STATEMENT
Approved for public release; distribution is unlimited.

12b. DISTRIBUTION CODE

13. ABSTRACT *(maximum 200 words)*

This thesis develops a model in Silvaco International's Virtual Wafer Fabrication (VWF) environment to assist advanced solar cell developers in designing more efficient solar cells intended for use in space. The complete model is intended to accurately predict the properties and characteristics of an existing state-of-the art multiple junction solar cell. This model should also be robust yet flexible in order to facilitate future modification and expansion. A specific dual junction cell, constructed of $GaInP_2/GaAs/Ge$ and displaying 24-26% efficiency at Air Mass Zero sun equivalency, was chosen as the baseline for this model and the characteristics of this cell and the materials that comprise it are explored and discussed. Basic building block models are constructed and displayed. Additionally, the intended structure of the eventual model is displayed and possibilities for future work are described.

14. SUBJECT TERMS
Solar Cells, Indium Phosphide Related Materials, Semiconductor Computer Modeling, Gallium Arsenide Related Materials, Silvaco

15. NUMBER OF PAGES
87

16. PRICE CODE

17. SECURITY CLASSIFICATION OF REPORT	18. SECURITY CLASSIFICATION OF THIS PAGE	19. SECURITY CLASSIFICATION OF ABSTRACT	20. LIMITATION OF ABSTRACT
Unclassified	Unclassified	Unclassified	UL

NSN 7540-01-280-5500

Standard Form 298 (Rev. 2-89)
Prescribed by ANSI Std. 239-18

Approved for public release; distribution is unlimited

HIGH EFFICIENCY SOLAR CELLS: A MODEL IN SILVACO

Darin J. McCloy
Major, United States Marine Corps
B.S.G.E., United States Naval Academy, 1987

Submitted in partial fulfillment of the
requirements for the degree of

MASTER OF SCIENCE IN ELECTRICAL ENGINEERING

from the

NAVAL POSTGRADUATE SCHOOL
September 1999

Author: _____
Darin J. McCloy

Approved by: _____
Sherif Michael, Thesis Advisor

_____
Ron Pieper, Second Reader

_____
Jeffrey B. Knorr, Chairman
Department of Electrical and Computer Engineering

ABSTRACT

This thesis develops a model in Silvaco International's Virtual Wafer Fabrication (VWF) environment to assist advanced solar cell developers in designing more efficient solar cells intended for use in space. The complete model is intended to accurately predict the properties and characteristics of an existing state-of-the art multiple junction solar cell. This model should also be robust yet flexible in order to facilitate future modification and expansion. A specific dual junction cell, constructed of $GaInP_2$/GaAs/Ge and displaying 24-26% efficiency at Air Mass Zero sun equivalency, was chosen as the baseline for this model and the characteristics of this cell and the materials that comprise it are explored and discussed. Basic building block models are constructed and displayed. Additionally, the intended structure of the eventual model is displayed and possibilities for future work are described.

TABLE OF CONTENTS

I. INTRODUCTION 1

A. BACKGROUND 1
B. OBJECTIVES 2
C. RELATED WORK 3

II. FUNDAMENTALS OF SOLAR CELLS 7

A. SEMICONDUCTOR THEORY 7
B. VALENCE BAND AND CONDUCTION BAND ELECTRONS 12
C. GENERATION AND RECOMBINATION OF ELECTRON-HOLE PAIRS 18
D. WAVELENGTHS AND BANDGAPS 23

III. MODELING OF SOLAR CELLS 27

A. GENERAL CONSIDERSTIONS FOR DEVICE MODELLING 27
B. SILVACO SPECIFICS, AN OVERVIEW OF SILVACO INTERNATIONAL SEMICONDUCTOR MODELING SOFTWARE 28

IV. MULTIPLE JUNCTION SOLAR CELLS 33

A. COST COMPARISON OF SOLAR CELL TECHNOLOGIES 35
B. RADIATION EXPOSURE ADVANTAGES OF MATERIALS IN MULTIJUNCTION CELLS 39
C. THE CASE FOR COMPUTER MODELS IN SUPPORT OF MULTIJUNCTION CELL DEVELOPMENT 42
D. DUAL JUNCTION BASELINE CELL TO MODEL 42

V. CONCLUSIONS AND RECOMMENDATIONS 49

A. CONCLUSIONS 50
B. RECOMMENDATIONS. 53

APPENDIX A. INPUT CODE FOR SINGLE JUNCTION SILICON CELL 55

APPENDIX B. INPUT CODE FOR DUAL JUNCTION CELL 59

APPENDIX C. INPUT CODE FOR SINGLE JUNCTION GaAs CELL 69

LIST OF REFERENCES 75

INITIAL DISTRIBUTION LIST 77

I. INTRODUCTION

Since the beginning of the space age, spacecraft have been powered by electricity generated from the sun's rays through the use of solar cells. The development of a better and more affordable cell has been a constant process of improvement ever since. By leaps and bounds and sometimes infinitesimal steps, the efficiency of solar cells has improved to the point we are at today.

A. BACKGROUND

The most common design of a solar cell from the outset of solar power was a single layer cell, usually consisting of silicon. Silicon is a common semiconductor material and benefits from years of experience in the semiconductor industry. The manufacturing and operating characteristics of silicon are well known and highly advanced in the industry as well. A solar cell made from silicon is limited in it's efficiency and the radiation tolerance of silicon is somewhat limited compared to other more exotic semiconductor materials.

As space missions grew more complex and of longer duration the drive to improve the efficiency and durability of solar cells and solar arrays as a whole was ever increasing. By producing a cell that was composed of various layers of dissimilar semiconductor materials, a multijunction cell, more voltage can be produced compared to a single layer cell made of any one of the component materials.

Multijunction solar cells have been an area of intense interest and study for the last decade or more. The references in the literature are rich and some important and

remarkable strides have been made in the last few years. Some of the more relevant studies are referenced at length in the following Chapters.

B. OBJECTIVES

This thesis seeks to develop a model to be used and expanded in the future to assist advanced solar cell developers make a better solar cell. A complete model is ideally intended to be accurate to the tested results of an existing solar cell as provided by a program management office or cell manufacturer. This model should be robust yet flexible. The intent is that this model be available as a baseline for more advanced solar cell research and development. An apt model will be able to simultaneously handle the myriad variables involved in solar cell design. The model should allow ease in switching materials in an existing design in order to perform what-if type tests as well as the more detailed and subtle differences in device designs.

A specific cell was chosen to model in order to have a basic structure to emulate and raw results to compare to. The desire was to find the state of the art in solar cells in order that the model developed could be as close to state of the art as possible. This way, only modifications and/or additions would need to be made to the model in order to tailor its application to the next generation of solar cell development. Additionally, the state of the art in solar cells is imagined to be fairly complex at the outset, a model intended for future research and development efforts must already prove its ability to handle complex forms and intricate relationships between the many variables involved.

The choice of a simulation program was based on the experience of the author with the Silvaco International "Virtual Wafer Fabrication" (VWF) suite of simulation

products. Currently, the solar cell industry and the research community related to it use products such as PC1D to model solar cells. This product is only a one-dimensional simulation tool. Silvaco provides a tool that will simulate in two and/or three dimensions, immediately improving the ability of the solar cell developer to "see" the cell in a whole new light. This suite of simulation products is in extensive use here at the Naval Postgraduate School.

It should be noted that it appears that no one has used Silvaco before to model advanced solar cells. From conversations we had with industry and research personnel, Silvaco was not a familiar tool to them. From the experience of the personnel here at the Naval Postgraduate School, it was apparent that the Silvaco simulation software had the potential to add a great deal to the field of advanced high efficiency solar cell design. The author then looked into this area of research and discovered the general field of multi-junction cascade solar cell design.

C. RELATED WORK

With the help of Prof. Michael and some intense background research, the author discovered an exciting project underway at the Phillips Laboratory in Albuquerque, New Mexico. This project sought to produce multijunction cells in a manner that simultaneously provided the benefit of increased power production and efficiency but also capped costs at a reasonable level above the previous generation of single junction cells. Efficiency increases of approximately 35% over this previous generation were projected and already realized on small batches of test cells [Ref. 1].

This technology was deemed a desirable baseline to build a model from. The program managers provided a rough, not to scale diagram of the cell structures under consideration and some test cells for use by the Naval Postgraduate School. Further detailed information was not available as the cells were still under contract and the detailed manufacturing information was proprietary. This was not a stopping point as the literature is rich with references to the various components of this type of cell. As well, there are specific references in the literature to very similar cell structures. The author was able to compile a fairly strong database of information useful in the construction of a model of this device.

The construction of models of transistor type devices has taken considerable effort and several students have collaborated in order to build specific device models in the past. Likewise, the construction of the multijunction solar cell model is not likely to be completed by only one student. The effort is expected to span the efforts of several students. In that light, this thesis sets out to define certain background issues involved in developing this cell as well as construct various models of sub-components of the eventual multi-layered cell.

In Chapter II, the theory of semiconductors and solar cells will be explored in order to further understand the mechanisms that lead to an effective and efficient cell. Chapter III addresses the applicability of models and Silvaco modeling tools specifically. The reasoning behind the development of multijunction cells, to include specific references to the materials and construction of the baseline solar cell will be hi-lighted and illustrated in Chapter IV. This will provide an understanding of the research and development undertaken to date in this field. Chapter V will conclude the thesis with a

summary of the work done to date. Some of that work, to include the input code and some of the graphical results produced from the Silvaco software, are included in the Appendices.

Basic models provided by Silvaco are available to model simplistic Silicon based single junction solar cells. These models were first modified to provide the proper outputs required for comparison by the solar cell industry. Then these models were further modified to match expected outputs.

Finally, the results to date in the form of computer code and diagrams will be included to aid any future endeavors to further this projected goal. Explanation of some of the peculiarities is included with this portion. There were many lessons learned to get to this point and it is hoped that a clear understanding of these lessons can be passed on to students who may undertake this project.

THIS PAGE INTENTIONALLY LEFT BLANK

II. FUNDAMENTALS OF SOLAR CELLS

Solar Cells are a subclass of semiconductors. A general discussion of semiconductors will be advantageous to understanding the complex structure of the dual junction solar cells to be examined in this thesis.

A. SEMICONDUCTOR THEORY

By examining the basic building blocks of solar cells and semiconductors in general, a more concrete understanding of how a solar cell works and what makes one more effective or efficient than another will emerge. The basic factors to consider are the elements that make up the semiconductors, the atomic and electron level interaction between the elements involved and the basic mechanisms that produce a current in semiconductors in general and solar cells specifically.

What is a semiconductor? First, by looking at the name semiconductor we get our first clue. In terms of conductance, semiconductors rank somewhere between a conductor and an insulator. The elemental semiconductors are Silicon (Si) and germanium (Ge), both group IV elements, found in column IV of the periodic table as shown in figure 1.

Compounds made up of two elements equally spaced away from the group IV elements also make-up some of the less common but very useful semiconductors. For example, Gallium (Ga) from group III and Arsenic (As) from group V together make a very useful semiconductor, Gallium Arsenide (GaAs), with many qualities superior to silicon or germanium. Compounds composed of elements from both column III and column V are commonly referred to as III-V compounds or materials. The expense of

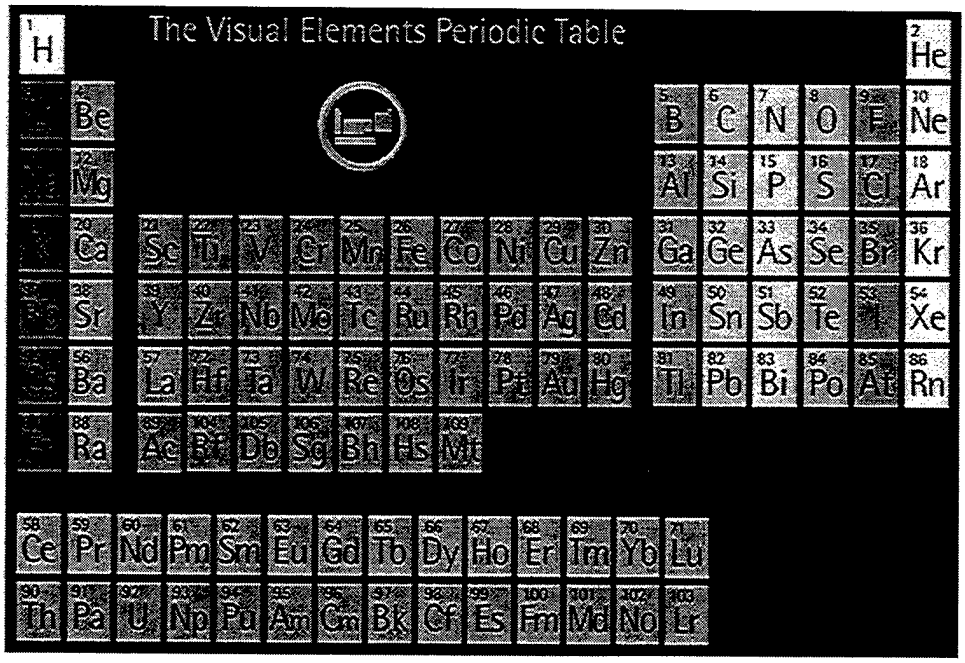

Figure 1. The Periodic Table of the Elements [Ref. 2]

manufacturing generally limits this and other compound semiconductors to niche markets where their unique qualities can be most effectively utilized. Semiconductors can also be made from 3 or more different elements, such as Indium Gallium Arsenide (InGaAs). In any combination of elements to make a semiconductor material, the resulting compound must have an average of four electrons in the outer band of each atom. This statement is critical to crystalline bonding and carrier movement characteristics in all semiconductors.

An atom with 4 electrons in the outer band, such as Si or Ge, will tend to share an electron with the 4 nearest neighbors, thereby giving that atom in the center the effect of having 8 electrons in the outer band. Figure (2) is a two dimensional model illustrating this point. The arrows emanating out from each atom represent the four outer electrons.

Si or Ge form a crystal lattice structure known as a diamond lattice. A unit cell of this type structure is shown in Figure (3).

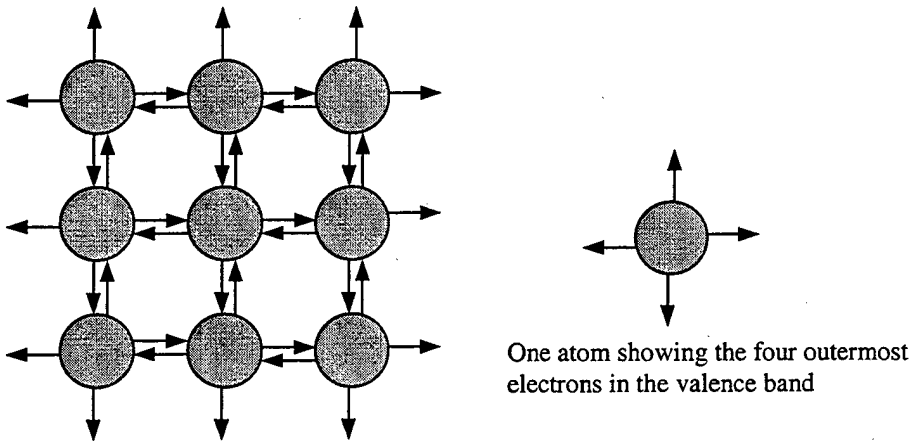

Figure 2. Two dimensional model of atoms sharing valence electrons [After Ref. 3]

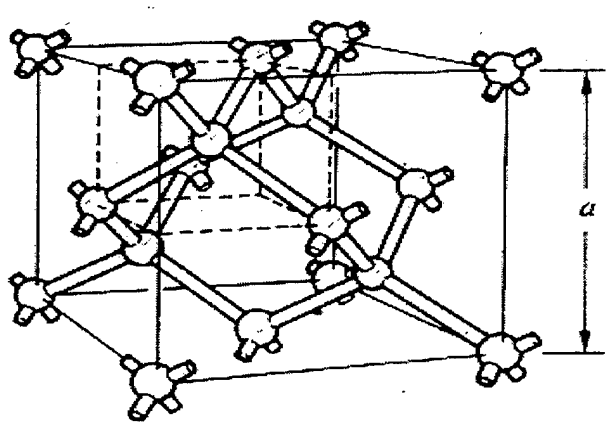

Figure 3. Diamond Lattice Unit Cell [Ref. 2]

A unit cell is the basic building block of a crystal lattice. By stacking multiple unit cells of the material of interest in three dimensions, we can visualize how the crystal lattice is arranged.

A semiconductor compound made from two or more elements will have atoms arranged in such a physical array and in such ratios to one another that each atom will share atoms with nearest neighbors to achieve an apparent 8 atoms in the outer valence band. Gallium and Arsenic will combine to form Gallium Arsenide (GaAs). Gallium has three valence electrons while Arsenic has five, an average of four per atom as gallium and arsenic are combined in equal parts. The atoms in GaAs will share electrons and arrange themselves into a crystal structure commonly referred to as a Zincblende lattice. A unit cell of the zincblende lattice is shown in Figure 4.

This figure shows the evenly and symmetrically arranged atoms of the compound

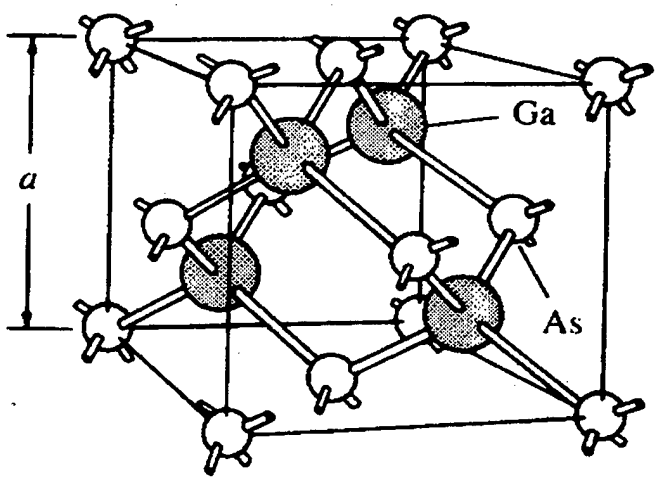

Figure 4. Zincblende lattice unit cell (GaAs) [Ref. 3]

and illustrates the difference in relative size of the Ga and As atoms. Because of this size mismatch, the GaAs lattice cannot form a diamond lattice like a single element semiconductor would.

There are four gallium atoms completely contained in the cell while the arsenic atoms are shared with other cells. The incomplete connections on the arsenic atoms in this figure indicate the bonds that would be made with gallium atoms of adjacent unit cells. Note that only 1/8 of each of the corner As atoms are actually contained in the unit cell while ½ of each of the face centered As atoms are contained in the cell. By adding up the eight corner atom portions with the 6 face centered portions we get four As atoms, confirming the even quantities of each element in the compound semiconductor.

To produce the ordered lattice arrangement of semiconductor crystals requires an extremely pure source material. The purity of the material used to manufacture semiconductors is crucial for two reasons. First, the amount of unintentional impurity will affect the crystalline structure of the semiconductor and cause unpredictable and undesirable results. Secondly, the amount of intended impurity or "dopant" determines the electrical properties of the semiconductor and therefore allows us to adjust some electrical characteristics of a material to meet our specific needs.

As mentioned before, the structure or arrangement of the atoms within the semiconductor lattice is crucial to the performance of the semiconductor final material. Three different categories of structure, amorphous, polycrystalline and crystalline, are used to describe the possible arrangement of atoms in semiconductors. As the names imply, amorphous material has no organization nor order, polycrystalline material is made up of many sections of perfect ordered atoms connected together with no predictable alignment between sections, and crystalline material is made up entirely of one continuous ordered crystal lattice. All three types are used in semiconductors but crystalline is by far the most common [Ref. 3]. As expected, it is also the most difficult

to manufacture. Ultrapure crystals, made up of continuous, predictably arranged atoms, are required for semiconductor manufacturing.

Obtaining an ultrapure crystal is no easy matter. Silicon, the most commonly used semiconductor material, does not occur naturally alone [Ref. 3]. It is only found as a part of a number of compounds. The process of purifying the material and growing the correctly structured crystals is long and tedious. Ingenious and varied processes have been developed to separate the desired elements from their natural compounds.

B. VALENCE BAND AND CONDUCTION BAND ELECTRONS

Bonding of semiconductor atoms is of interest to us but does not completely explain the interactions between the atoms that give rise to the desired properties of the semiconductor in general and the solar cell specifically. In order to fully understand those properties we must also look at the energy-related properties of the semiconductor atoms and electrons.

For the silicon atom, used here as an example of a simple model, the 14 electrons are arranged in three distinct energy bands around the nucleus. The inner band contains two electrons and the next band contains eight. The remaining four electrons occupy the outermost band that is the most weekly bound to the atom. The inner 10 electrons are tightly bound to the nucleus and are not likely to be perturbed by any interaction between atoms. The outer four on the other hand are affected greatly by this interaction. In an atom that is isolated from other atoms (that is, far enough away so that they do not interact with other atoms) the outermost four electrons would occupy the lowest energy states of the outer band [After Ref. 3].

As a number of Si atoms are brought closer together, the allowed energies begin to spread as a result of the interatomic forces. Once the atoms are closely aligned, as in the lattice spacing of a typical crystal, the allowed energies form two distinct energy sub-bands separated by an energy gap. The upper and higher energy band of allowed states is called the conduction band and the lower band is called the valence band. The conduction band is named such because electrons in this band add to conduction as they are more likely to break free and become charge carriers. The energy gap between these bands is the band gap as shown in Figure 5. In general, electrons tend to

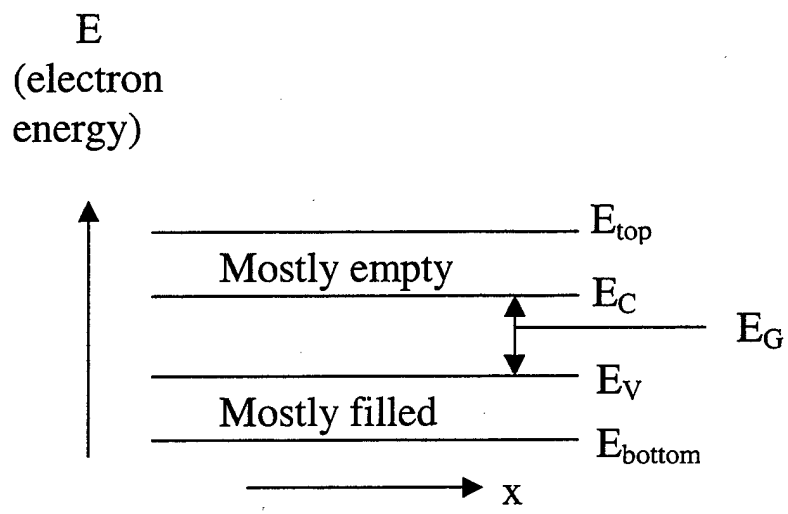

Figure 5. Energy bands and band gap [After Ref. 3]

fill the lower energy or valence band first. In the silicon atom, the outer band can only accommodate 8 electrons, 4 in the valence band and 4 in the conduction band. The energy or band gap of a material serves to distinguish it as a conductor, semiconductor, or insulator [Ref. 3].

As we just mentioned, energy levels and energy level differences determine the arrangement of electrons around the outer band in the atom. The energy or force with which the electrons are bound to the atom are of interest and will prove crucial as the characteristics of solar cells are examined. Known as bandgap energy, it varies from one semiconductor material to another and is affected/determined by the size of the atom and the number of electrons in the valence band. For silicon, the bandgap energy of a free donor electron is E_G= -1.1eV. In effect, an externally applied force equal to or greater than the bandgap energy of a free donor will break the electron free from the conduction band. This action creates an electron free to roam about the lattice, as well as a hole, or absence of an electron that also can roam about the lattice.

What makes a semiconductor a conductor at all is the movement of charge from place to place. The alignment of the individual atoms ensures an equal number of holes and electrons in an ideal intrinsic crystal. A pure, homogeneous semiconductor material is considered intrinsic. It contains only the element (or elements in the case of compound semiconductors) intended to form the semiconductor crystal lattice.

A doped semiconductor, on the other hand, has an intentionally added material that serves to manipulate the predominant carrier concentration. In intrinsic semiconductors the number of holes and electrons are equal since the creation of a free electron necessarily creates a hole in its absence in the atom to atom bond structure. By adding material from column III of the periodic table (boron for example) we create an overall p-type material. The three electrons of the boron atom will bond to adjacent Si atoms but leave one possible bond undone. In essence, this creates a local positive charge or hole. Hence, p-type material with more holes than electrons. A hole is the

absence of an electron so therefore a net positive charge equal in magnitude to an electron charge is formed when a hole is formed [Ref. 4]. Figure 6(b) shows a two

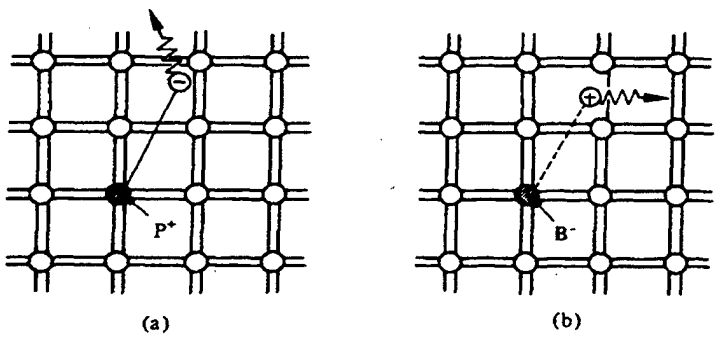

Figure 6. Donor and acceptor action [Ref. 3]

dimensional example of the introduction of a Boron atom into a Silicon lattice.

Conversely, by adding a material from column V an n-type material is created. The column V material (phosphorous for example) bonds with the four nearest neighbor Silicon atoms, leaving one electron of the five in the outer band unbonded. This excess electron is a carrier and a net negative charge free to roam about as in figure 6(a) [Ref. 4].

Doping concentrations directly effect the number of free electrons or free holes per cm^3 of semiconductor material. While there will always exist a number of free electrons and holes in a material due to thermal generation, the effect of doping is to manipulate the concentration of one carrier type over the other.

1. pn Junctions and Diffusion Current

When an area of n-type material is brought into contact with an area of p-type material a pn junction is formed. This junction is in effect a diode. Electrons from the n-

type material diffuse into the p-type material and combine with holes. Likewise, holes from the p-type material diffuse into the n-type material and recombine with electrons. This diffusion creates a current, diffusion current. The diffusion of these carriers away from their respective type materials creates a region of depleted charge in an area close to the actual layer junction, a depletion region. The depletion region induces an electrical potential in the opposite direction of the diffusion current. As the diffusion current increases, the electrical potential across the depletion region increases and eventually equilibrium is reached [Ref. 4].

2. Drift Current

In addition to the majority charge carriers that create the diffusion current, minority charge carriers interact with the junction to create drift current. Minority carriers on both sides of the pn junction drift randomly in the lattice structure. When the hole minority carrier in the n-type material interacts with the depletion region, the electric field of the depletion region will sweep the hole to the p-type side of the region. Conversely, when the electron minority carrier in the p-type region interacts with the depletion region, the field will sweep it to the n-type region. These two currents combine to make the drift current. With no external bias applied and when the cell is dark, the drift and diffusion currents are equal and opposite.

Carrier mobility is also of interest. Generally, electrons are more mobile than holes. Mobility, measured in standard units of $cm^2/V\text{-}sec$, is the central parameter in characterizing hole and electron drift.

Drift is the motion of charged particles in response to an electric field. As shown in figure 7(a), an applied electric field has the affect of forcing positively charged holes in the direction of the electric field while the negatively charged electrons are forced to

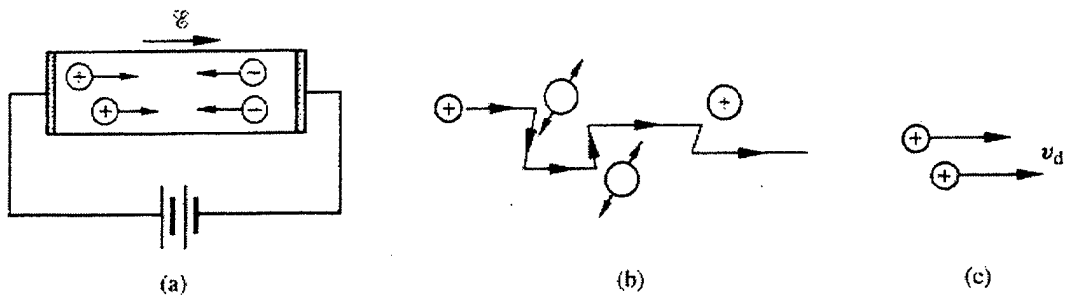

Figure 7. Carrier Drift: (a) motion of carriers in biased semiconductor bar; (b) drifting hole on a microscopic scale; (c) carrier drift on a macroscopic scale. [Ref. 3]

move in the opposite direction of the field. The carriers move in the general direction of positive and negative field lines but on a microscopic scale are subject to many decelerations and subsequent accelerations as they collide with other lattice atoms and are then again forced to move by the electric field as shown in figure 7(b). The result is scattering. On the macro scale, in figure 7(c), the sum of all of these motions, scattering and collisions is the constant drift velocity, v_{dn} [Ref. 3].

3. Total Diode Current Under Illumination

The total diode current of an illuminated solar cell is a combination of light-generated current and the dark current. The dark current of a solar cell is the same as the dark current characteristics of any diode in that it is the combination of diffusion current, drift current and shunt current. Equation 1 is the total diode current under illumination

$$I = I_L + I_S\left[1 - \exp\left(\frac{V + R_S I}{m_{id} V_{th}}\right)\right] \qquad (1)$$

where the second term on the right hand side of the equation is the dark current, I_s is the dark saturation current, V is the applied voltage, m_{id} is the diode ideality factor, and R_S is the diode series resistance. [Ref. 5]

The built-in electric field generated by the pn junction can at most provide the built-in potential. This built-in voltage is the upper limit of open circuit voltage (V_{OC}). In order to produce a higher V_{OC}, cell designers ensure a stronger field across the pn junction by increasing the doping differential across the junction. A p^+n or n^+p junction will have a higher possible V_{OC} than a straight pn or np junction. Additionally, the top layer, whether p+ or n+, is made very thin because the diffusion layer in highly doped layers is very small [Ref. 5].

C. GENERATION AND RECOMBINATION OF ELECTRON-HOLE PAIRS

There are three basic generation and recombination mechanisms for electron hole-pairs. They are (1) auger, (2) radiative, and (3) thermal.

1. Auger generation recombination

An Auger event is one in which a high-energy particle or free carrier impacts a crystal lattice and the energy from that particle is imparted onto an electron in the lattice, thereby breaking it free of the lattice. Commonly referred to as impact ionization, this event creates an electron-hole pair. For Auger recombination, an electron-hole pair recombines, transferring the energy from that recombination to a free carrier in the lattice, which is then excited to high energy within the band [Ref. 6].

2. Thermal generation/recombination

Thermal generation and recombination is ever present and explains the presence of free carriers in an intrinsic semiconductor under equilibrium conditions with no outside forces or biasing applied. In thermal generation, as shown in Figure 7(a), a free electron-hole pair is formed when thermal energy is transferred to an electron in the lattice in the form of a phonon. The reverse is true of recombination; an electron-hole pair recombines and transfers the energy to the lattice in the form of a phonon. At 300° K (room temperature) thermal generation alone creates approximately 1.5×10^{10} free electrons and an equal number of holes moving freely about in one cubic centimeter of pure silicon.

3. Photogeneration

Last and of most importance to this paper is radiative generation. Band-to-band optical generation and recombination events are radiative and occur due to photon absorption or emission respectively. Figure 8(b) illustrates such generation and recombination mechanisms [Ref. 6].

This illustration is accurate only in the case where there is direct conversion of the photon to a free carrier or vice versa. In cases where there are unintentional impurities in the lattice and/or the semiconductor is an indirect-gap material, the actual generation and recombination events differ significantly.

In an indirect-gap semiconductor the conduction band minimum and the valence

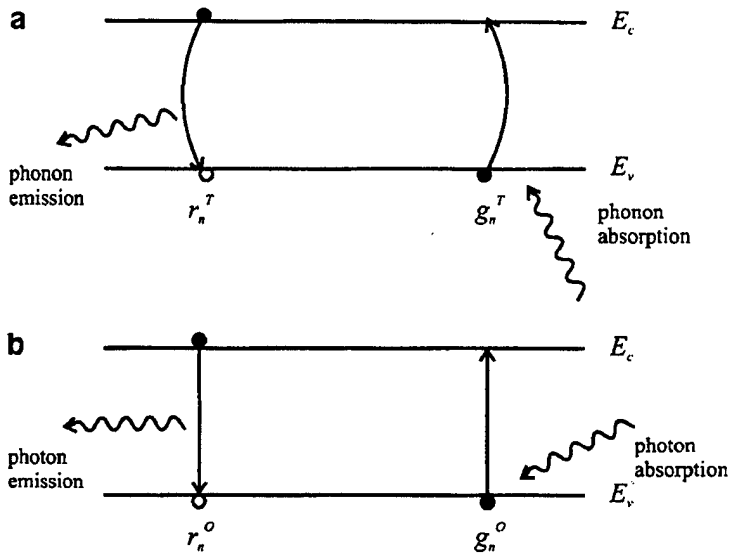

Figure 8.(a) Thermal generation/recombination, (b) Radiative Generation/Recombination [Ref. 6]

band maximum (hole-energy minimum) occur at different points in k space as shown in Figure 9. The electron k vector is crystalline momentum and k space is often referred

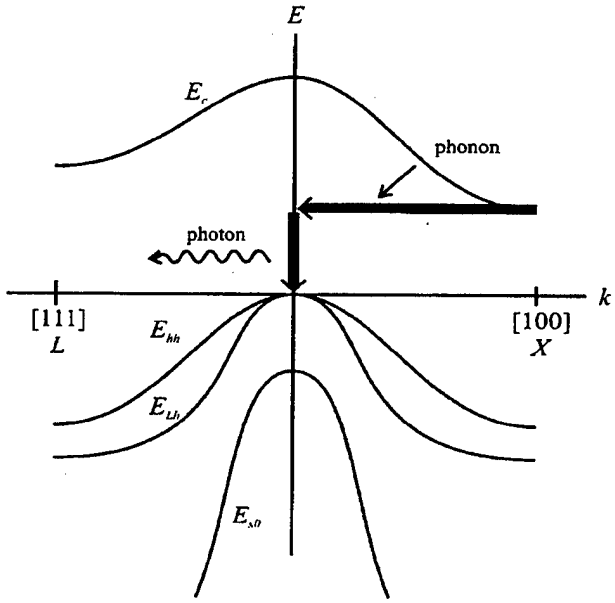

Figure 9. Indirect bandgap material [Ref. 6]

to as reciprocal lattice space since it has units of inverse length. A more extensive and complex review of this concept is not entirely necessary here but the reader is directed to Brennan, Ch. 8 [Ref. 6] for a concise explanation.

In addition to indirect-gap materials, materials with defects or impurities will act as indirect gap materials due to the effect of the defects. In the case of indirect-gap materials such as silicon or germanium, the photon in a generation case must first excite an electron in the lattice to a higher energy state within the band. In effect, creating a phonon. This phonon then directly creates a free carrier. The reverse is true for recombination. This, in effect is a second-order transition [Ref. 6].

Direct-gap materials exhibit a conduction band minimum and the valence band maximum at the same point in k space as shown in figure 10. For direct gap materials

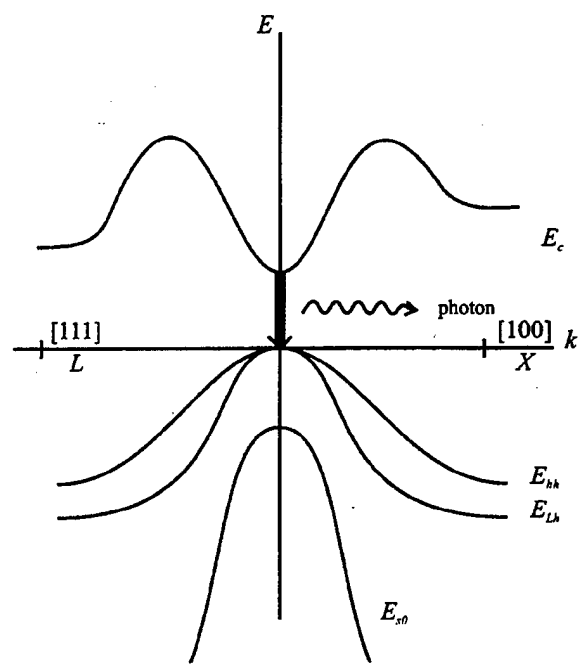

Figure 10. Direct bandgap material [Ref. 6]

such as GaAs, InP, ZnS, a photon is directly converted into a free carrier without an intermediate step, hence the term, direct-gap. In the case of direct semiconductors, the energy and momentum are conserved during optical generation and recombination events.

A first order transition, such a direct-gap, occurs according to Fermi's golden rule [Ref. 6]:

$$W = \frac{2\pi}{\hbar}\left|\langle k|V|s\rangle\right|^2 \delta(E_k - E_s) \qquad (2)$$

Where V is the perturbing potential that instigates the transition, h is Planck's constant, s is the initial state, k is the final state, E_s is the energy at the initial state, and E_k is the energy at the final state. In optical radiative events, V is the electric dipole moment. The probability that such a transition in this case will occur depends on the square of the matrix element <k|V|s>.

The second order transition rate of the indirect-gap semiconductor radiative recombination occurs according to equation 3 [Ref. 6]

$$W = \frac{2\pi}{\hbar}\left|\sum_m \frac{\left(\langle k|V|m\rangle\langle m|V'|s\rangle\right)}{(E_s - E_m)}\right|^2 \delta(E_k - E_s) \qquad (3)$$

where m is an intermediate step, E_m is the energy at that intermediate state, and V' is the perturbing potential required to move from the intermediate state to the final state. The transition in this equation occurs from initial state |s> to an intermediate state |m> and then to the final state |k>. The intermediate state is mediated by a phonon event. It is important to note that the intermediate state |m> and the final state |k> are at the same point in k space.

The total probability that the indirect transition will occur at all depends on the probabilities of either state event occurring. The probability that a second order transition will occur is much less than that for a first order transition. For generation, an incident photon may succeed in forcing a transition from initial state (electron in conduction band) to intermediate state (electron in higher energy state but still in conduction band). But if the transition to final state (free electron hole pair) is not reached the result is a phonon or heat added to the lattice and no additional current produced [Ref. 6]. For this reason, direct-gap semiconductors are considered more efficient photoelectric devices than indirect semiconductors.

The relative ease with which silicon is processed and the relatively low cost of silicon as compared to the direct-gap materials certainly explains silicon's dominance of the commercial photoelectric field up until recently. As will be illustrated later, the efficiencies of direct energy gap materials are being taken advantage of to overcome the cost differential. As the explosion of space based communication resources continues, more and more cost effective and reliable components of satellite systems are being developed and readied for the marketplace.

D. WAVELENGTHS AND BANDGAPS

Radiative generation is the basic phenomenon behind the solar cell. Light captured or absorbed by a semiconductor cell is in essence converted into free electron and hole carriers in the cell. These free carriers must then be "collected" before they have a chance to recombine. In a cell with no outside connections the free electrons and

holes would eventually recombine. By doping the cell to form a pn junction, the charges can be separated and collected by metal contacts on the top and bottom of the solar cell (as in figure 11).

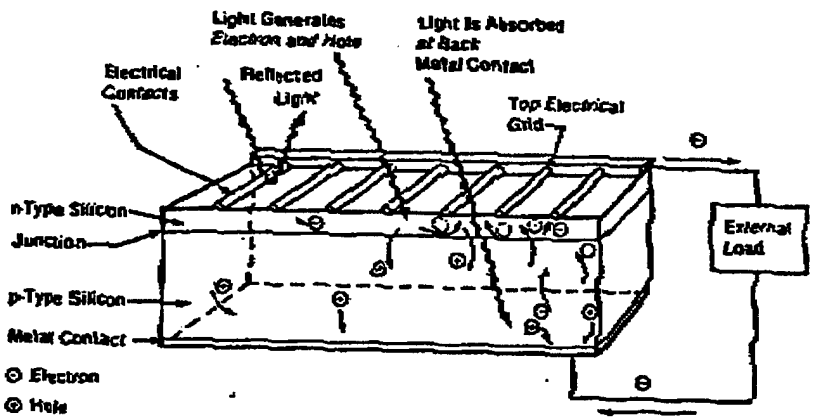

Figure 11. Basic Silicon Solar Cell Operation [Ref. 7]

As mentioned earlier, each semiconductor material has a specific bandgap energy. This energy level determines the minimum energy required in the form of ionizing radiation, thermal energy (or phonons), or in the case of solar cells, photon energy, to break an electron loose from the conduction band of an atom in the crystal lattice. In solar cells, the crystal lattice is in fact bombarded by photons from the sun. The photon energy Ep can be determined with equation 4 [Ref. 6].

$$E_p = h \times v = h \times \left(\frac{c}{\lambda}\right) = \frac{1.24}{\lambda} \tag{4}$$

Where $h \times v$ is energy in electron volts (eV), h is Plank's constant, v is frequency of light wave, c is the speed of light and λ is the light wavelength in micrometers (μm).

Therefore, light of wavelength y (μm) will only produce free electron hole pairs in a semiconductor if 1.24/y is equal to or greater than the bandgap energy of the

semiconductor material in question. For a material of bandgap x eV, that corresponds to a wavelength of light y μm, any wavelength greater than y is absorbed in the material while wavelengths less than y are more energetic and therefore pass through the cell nearly unperturbed.

THIS PAGE INTENTIONALLY LEFT BLANK

III. MODELING OF SOLAR CELLS

The author was unable to find in the literature any reference to the use of Silvaco software to model solar cell characteristics. Several other software products were encountered in the literature, the most common being PC1D. Silvaco has several qualities that lend itself to the modeling and simulation of solar cell devices in an effort to more cost effectively explore the possibilities of new and complex designs for ever increasing productivity and efficiency of solar cells. Silvaco is in use at the Naval Postgraduate School in Monterey by a number of students and professors but almost exclusively in support of research of transistor devices.

A. GENERAL CONSIDERSTIONS FOR DEVICE MODELLING

To model single layer or homogeneous solar cells a mathematical model must take into account the following:

1) drift and diffusion currents
2) position dependent doping
3) doping dependent mobility
4) optical carrier generation
5) bulk generation-recombination effects
6) surface recombination effects

By complicating the modeling problem with spatially varying parameters the following factors must then be considered:

1) position-dependent bandgap

2) position-dependent electron affinity

3) built-in fields due to varying bandgap

4) composition-dependent refractive index

5) heterojunction interface recombination

6) other position dependent material parameters such as mobility, dielectric constant, and optical absorption coefficient [Ref. 8]

B. SILVACO SPECIFICS, AN OVERVIEW OF SILVACO INTERNATIONAL SEMICONDUCTOR MODELING SOFTWARE

Silvaco International provides a software product that models the behavior of semiconductor materials, devices, and circuits using finite element techniques. This software is useful in this case because it can be programmed to build or grow a semiconductor crystal in a "Virtual Wafer Fab" facility and then determine electrical characteristics of that device once initial biasing conditions are inputted. By actually growing the device just as a fabrication line would, the user can experiment with the myriad procedures available to the process designer and therefore identify the most effective and cost efficient process for production purposes [Ref. 9].

There are many programs/tools within Silvaco. Each tool supports a different area within semiconductor device modeling and most are able to directly interact with each other. The most important tools to this paper are ATLAS, ATHENA, and Luminous.

ATLAS is the basic tool that provides the general capabilities for numerical, physically based, one, two, or three-dimensional simulation of semiconductors. ATLAS

is the overarching architecture and includes many tools that simulate various devices and specific conditions of operation.

Among the specific device simulation tools are:

S-PISCES, to simulate silicon devices;

BLAZE, to simulate arbitrary semiconductors and heterojunction devices;

GIGA, that allows the simulation of non-isothermal conditions;

TFT, to simulate polycrystalline and amorphous materials;

LUMINOUS, simulates optoelectronic devices;

LASER, to simulate heterostructure lasers;

MIXEDMODE, circuit simulation tools that employ both numerical physically based devices and compact analytical models;

as well as others [Ref. 9].

Luminous provides the most obvious benefit to the subject of this thesis. With this module of Silvaco the user is able to subject various semiconductor devices to light energy in specific wavelengths and intensities. The user specifies the incidence angle, polarization, range of wavelengths, intensity and origin o the light source. Figures 12 and 13 show some advanced device simulation graphical results from luminous.

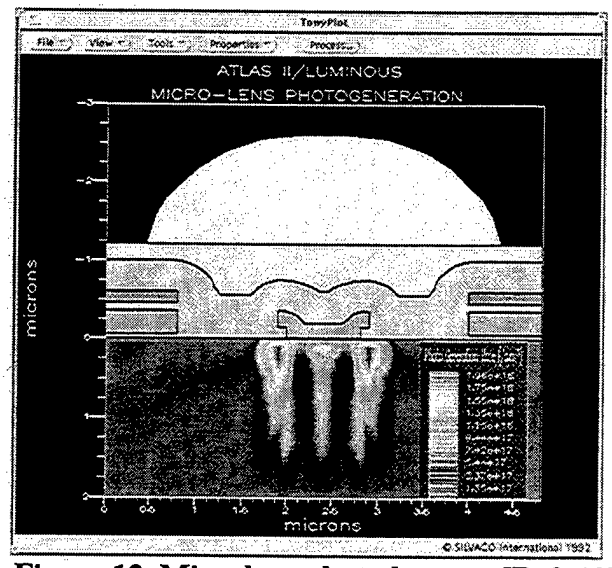

Figure 12. Microlens photodetector [Ref. 10]

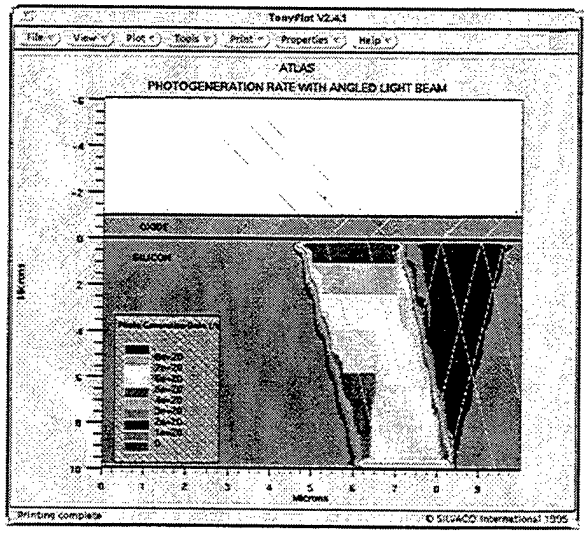

Figure 13. Photogeneration rate in a solar cell [Ref. 10]

Physically-Based Simulation

Physically-Based Simulation is advantageous for semiconductor device simulation. According to the ATLAS User's Manual,

> Physically-based device simulators predict the electrical characteristics that are associated with specific physical structures and bias conditions. They do this by solving systems of coupled, non-linear partial differential equations that describe semiconductor physics.
>
> Physically-based simulation provides three major advantages; it is predictive, it provides insight, and it captures theoretical knowledge in a way that makes this knowledge available to non-experts.
>
> Physical-based simulation is different from empirical modeling. The goal of empirical modeling is to obtain analytic formulae that approximate existing data with good accuracy and minimum complexity. Empirical models provide efficient approximation and interpolation. They do not provide insight, predictive capabilities, or encapsulation of theoretical knowledge. Physically based simulation is an alternative to experiments as a source of date. Empirical modeling can provide compact representations of data from either source.
>
> Physically based simulation has become very important for two reasons. First, it is almost always much quicker and cheaper than performing experiments. Second, it provides information that is difficult or impossible to measure. The drawbacks of simulation of that all the relevant physics must be incorporated into a simulator, and numerical procedures must be implemented to solve the associated equations. The tasks have been taken care of for users of ATLAS. [Ref. 9]

Users of physically based device simulation tools must specify the problem to be simulated. Users of ATLAS specify device simulation problems by defining:

1. The physical structure to be simulated
2. The physical models to be used
3. The bias conditions for which electrical characteristics are to be simulated.

   [Ref. 9]

The physical structure can be defined in several ways. The most visually obvious method is by using the DEVEDIT package to actually draw a device region by region. In DEVEDIT, the size of the individual regions are dictated as well as the materials that make them up. In order to perform tests on a device designed in DEVEDIT, the structure and input commands must be saved and then read into the DECKBUILD application.

Upon opening the DECKBUILD application, the user must load the input file (*.in) for the specific device designed and saved in DEVEDIT. DECKBUILD then displays a list of commands in a text file format that DEVEDIT converted from graphical structure. The commands specify the specific size and shape of the device "work area" and each individual region in verbal and numerical terms. Specific materials, as specified in DEVEDIT, are included in this textual description of the device as well as the grid or mesh desired by the user.

All factors imported from DEVEDIT to BECKBUILD can also be modified once in DECKBUILD. Additionally, the entire structure can be indicated from the DECKBUILD window originally, bypassing altogether the DEVEDIT step. Certain advantages exist for either method. In the author's opinion, novice users may well be served by initially designing a device in DEVEDIT. The DEVEDIT widow provides myriad pull-down menus and is generally more quickly mastered than the complex and time intensive method of manually inputting design criteria in a text format. A more experienced user will most likely prefer a mixture of both methods. By using DEVEDIT to first setup the general physical size and shape of a device, the more experienced user can then import it into DECKBUILD and modify and add the more detailed steps involved.

In either case, a general knowledge of UNIX operating systems is advantageous to the SILVACO user. File manipulation, importing and exporting graphs and input lists, and general use of the networked system will prove crucial to getting the most in the from of results and useable products from your many hours of effort invested.

IV. MULTIPLE JUNCTION SOLAR CELLS

In order to build a model that is as close as possible to cutting edge research and development we chose a recently produced cell that is still under development. The focus of the computer model for this project is a dual junction cell consisting of active layers of GaAs and $GaInP_2$ on a germanium substrate. The active layers are connected by tunnel diodes made of GaAs and there are window layers composed of $GaInP_2$ and $AlInP_2$.

While silicon is the most common semiconductor material and is by far the predominate material used for solar cell production it displays a marked vulnerability to the severe environment of space. Most notably of its susceptibilities is its relative radiation intolerance. Several other common semiconductor materials as well as some not so common "exotic" semiconductor compounds have been shown to display far superior radiation tolerance characteristics.

Additionally, these materials display generally much higher efficiencies under Air Mass Zero (AM0) sun conditions than even the most advanced silicon space cells. By taking advantage of various bandgap materials and stacking those materials in the best possible configuration, developers have been able to demonstrate some very impressive performances in optimized cells. By first discussing some of these materials and providing data to support their claims to superior performance and endurance, the intent is to then show how one might from that information develop a stacked or multiple junction cell that possesses truly superior performance and reliability. In this project, a dual junction cell developed by Spectrolab is the baseline structure for the model to be

developed. Spectrolab, under contract with the Air Force Research Laboratory, Phillips Labs, at Albuquerque, NM, developed this cell as part of the ManTech program [Ref. 1].

The joint Wright Laboratory (Wright Paterson AFB), Phillips Laboratory (Kirtland AFB), and NASA (Lewis Research Center) Multijunction Solar Cell Manufacturing Technology (ManTech) program has as its ultimate goal the scale up of GaInP2/GaAs/Ge multijunction solar cells to production size, quantity and yield. This capability was to be achieved while maintaining a total manufacturing cost of only 15% over state of the art GaAs single junction cells (as measured in cost/W ($/W)). In a progress report presented at the Twenty-Sixth IEEE Photovoltaic Specialists Conference in 1997, progress toward "phase I" goals was discussed. Phase I goals were focused on the production scale up of cell size, yield and efficiencies. Phase II is to continue those efforts but mainly focus on the cost reduction [Ref. 1].

Results reported best cell efficiencies of 25.76% and 24.7% and lot average efficiencies of 24.2% and 23.8% from the two separate contractors involved. The lot average cell efficiency goal of the program is 24-26%. State of the art GaAs cells typically achieve lot average efficiencies of 18.5% [Ref. 1].

Comparison of solar cell efficiencies alone will not completely classify a particular cell's usefulness or cost effectiveness in a particular application. As mentioned in the preceding discussion, the goal of the ManTech program was to produce a multijunction cell that was 24-26% efficient but at he same time will cost only 15% more to manufacture. Manufacturing costs will figure prominently into overall acceptance of this new technology.

A. COST COMPARISON OF SOLAR CELL TECHNOLOGIES

In order to more accurately compare the costs and benefits of one cell type over another, an extensive trade study was performed by E. L. Ralph of the Applied Solar Energy Corporation. In this study the total system cost are considered in order to give the satellite system designer an accurate comparison baseline to aid in power system component selection. It was assumed that a mission destined for geosynchronous orbit was desired and that all cell sizes are 4cm by 4cm. The cost comparisons were performed on component then system level, starting with bare cell cost and performance characteristic data. In Table 1 the individual cell level characteristics are shown [Ref. 11].

CELL TYPES	BOL @ 28 C		EOL @ 60 C		CELL WEIGHT	CELL COST
	%	KW/m^2	%	KW/m^2	Kg/m^2	$\$K/m^2$
Si (200um)	12.6	.170	8.7	.118	.464	10
Si (67um)	15	.203	9.2	.124	.156	20
GaAs/Ge (137um)	18.5	.250	13.9	.188	.720	80
MJ Cascade (137um)	22	.298	16.5	.223	.720	96
MJ Cascade (137um)	25	.338	18.8	.254	.720	100
Thin Film	12.6	.170	9.5	.128	.100	10

Table 1. Component level cost of various solar cell technologies [After Ref. 11]

As is readily apparent from the above table, the more advanced and higher efficiency solar cells are significantly more expensive on a per cell basis. Where as the cost of more advanced systems and technologies is significantly higher than Silicon, the continually improving effectiveness of Silicon designs makes it more difficult to directly determine

which avenue is more efficient in terms of total system cost, cost to orbit, duration and operating environment concerns. A more comprehensive comparison, considering total solar array cost to support a baseline power requirement is needed to show true cost effectiveness.

It was determined that the costs and weights of the array structure were the same (per unit of area) for each separate technology as shown in Table 2.

WEIGHTS	Kg/m^2
Coverglass (150 um)	.397
Cover Adhesive	.067
Interconnects	.013
Cell Adhesive	.230
Bus/Wire/Diodes	.307
Substrate	1.144
Total (less Cells)	2.158
COSTS	**$k/m^2**
Coverglass	4.3
CIC Fabrication	3.5
Circuit Laydown	8.1
Subtotal Electrical (Less Cells)	15.9
Substrate/Integration	13.9
Mechanisms	11.5
Total Array (Less Cells)	41.3

Table 2. Solar Array Basic Assumptions [After Ref. 11]

The factors in Table 2 are the required and existing solar array construction component costs no matter what the cell design chosen.

Table 3 on the other hand, shows the effective cost per unit of power produced and weight of cells per unit of power produced. Obviously, a more efficient cell will require fewer cells to produce a set amount of power than a less efficient cell would.

In Tables 2 and 3 the end of life calculations and results are based on a radiation exposure of 1e15 e/cm^2 and an operating temperature of 60°C. As shown in Table 3, the

multijunction cells at both 25% and 22% efficiency have initial and end of life cost advantages over existing state of the art GaAs/Ge cell technology but are still edged out

CELL TYPES	BOL @ 28 C	WEIGHTS		COSTS		Δ WT VALUE $K/KW	Δ AREA VALUE $K/KW
		BOL Kg/KW	EOL Kg/KW	BOL $K/KW	EOL $K/KW		
Si (200um)	12.6	15.4	22.2	300	432	--	--
Si (67um)	15	11.4	18.7	300	492	231	20
GaAs/Ge (137um)	18.5	11.5	15.3	484	644	455	152
MJ Cascade (137um)	22	9.7	12.9	460	614	614	192
MJ Cascade (137um)	25	8.5	11.3	417	555	719	218
Thin Film (Si)	12.6	11.2	14.8	252	336	488	32

Table 3. Complete Array Weight and Cost Calculations [After Ref. 11]

by all three Silicon technologies displayed. As mentioned above, these results are for total solar power array costs and weights only.

But array construction costs alone are not an accurate measure of total array subsystem value. As seen in Table 3, the multijunction cell at 25% efficiency displays the best weight value, with the lowest weight per kW of power produced at beginning of life as well as end of life. In space operations, weight can be directly converted into costs in the form of launch and station keeping costs. Launch costs are typically set at about $11k/kg for low earth orbit and about $66k/kg for geosynchronous orbit [Ref. 11]. Once a satellite is in orbit, fuel must be expended to keep it in the right orbit. Drag from the spacecraft surface area and weight cause the spacecraft to slow down and/or drift to an undesirable orbit. The size of an array therefore has a direct effect on the station-keeping costs experienced over the lifetime of a satellite. A typical value of station-keeping fuel usage is 0.073kg/m^2/yr or an array cost reduction value of $48k/m^2 due to area reduction

for a 10 year GEO mission. These values were used to calculate the results in the last two columns of Table 3 above. Figure 14 shows the relative size difference to be expected when building a solar power array to supply a set power rating.

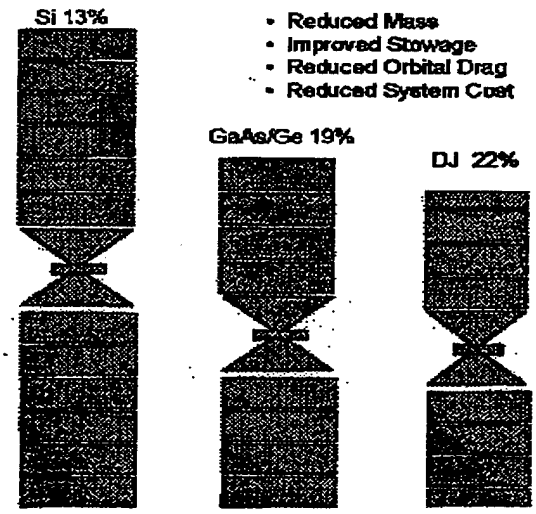

Figure 14. Relative Array Sizes for Various Cell Types [Ref. 12]

Another advantage not previously considered is the increase in capability in a satellite design due to higher power availability and/or more weight budget allocated toward payload electronics vice support subsystems. A revenue related cost factor was used to formulate the graph in Figure 15. A value of about $740k/kg is most likely justified if the added revenue from increased communications channels allowed by weight reduction/power increase of each cell type were considered.

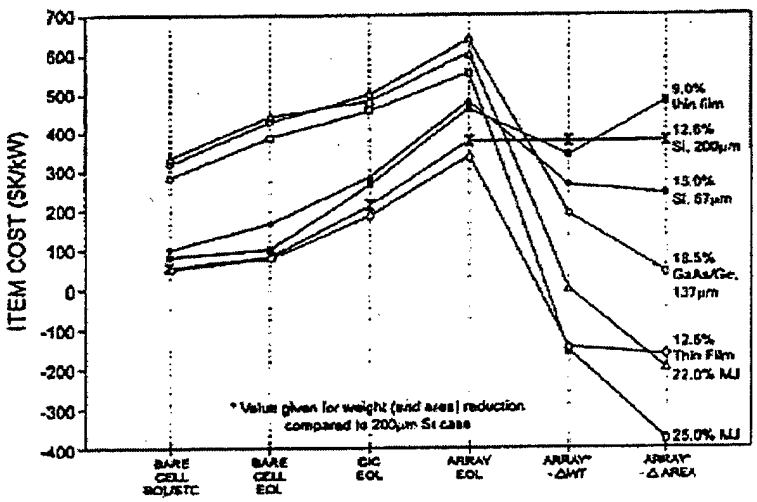

Figure 15. Cost to build Complete Array [Ref. 11]

This last chart is a clear indicator of the overall system level advantage to be gained by the use multijunction cells. In Figure 15 the dramatic and clear superiority of multijunction is shown. The drive to further improve the technology base of multijunction cells should be apparent. It is envisioned that operating efficiencies of as much as 33% can be realized with a quadruple layered cell. Current dual junction cells are achieving the 25% efficiencies used in the system trade-off study referenced above [Ref. 1].

B. RADIATION EXPOSURE ADVANTAGES OF MATERIALS IN MULTIJUNCTION CELLS

The materials that make up the multijunction cells are tuned to the available spectrum of light emanating from the sun but also show superior radiation tolerance to silicon. A typical multijunction solar cell contains Indium Phosphide as well as Gallium Arsenide based compounds. Both of these materials and their derivatives have been shown to display superior radiation tolerance to Silicon.

In a study that specifically focussed on dual junction p^+n InGaP/GaAs space solar cells, researchers from the Naval Research Laboratory and SFA, Inc found strong evidence to support this claim of radiation tolerance. In this test, they compared the beginning of life and end of life characteristics of the InGaP/GaAs cell to a single junction InGaP cell and a single junction GaAs/Ge cell as well as a n^+p InGaP/GaAs cell [Ref. 13].

Each of these cells were irradiated with either 3 MeV protons or 1 MeV electrons. Figure 16 shows the radiation response of the p^+n InGaP/GaAs (DJ) cell for 1 MeV electron fluences from zero to 10^{16} (cm^{-2}).

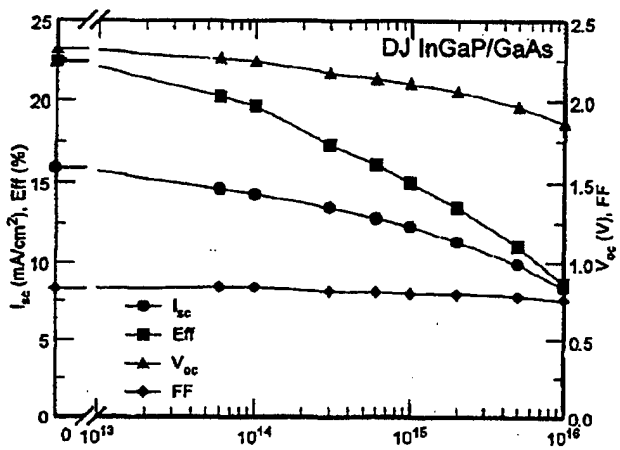

Figure 16. Response of DJ p^+n InGaP/GaAs cell to 1 MeV electron radiation [Ref 13]

Figure 17 shows the degradation of the single junction p^+n InGaP cell under the same type radiation ranges.

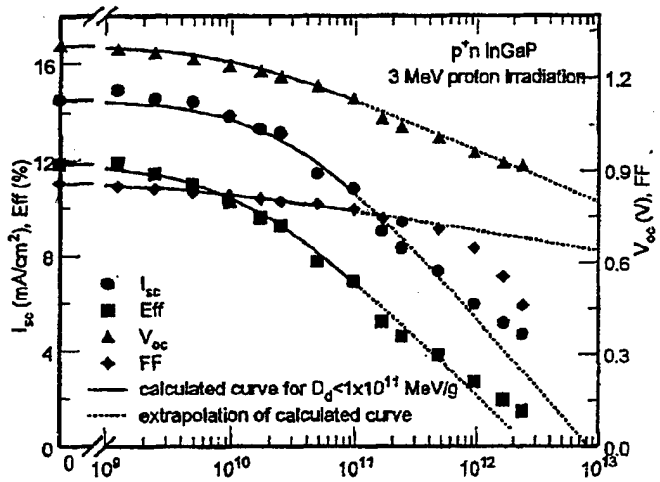

Figure 17. Response of SJ p^+n InGaP cell to 1 MeV electron radiation [Ref. 13]

All of the different technology type cells are compared on one graph in Figure 18. Notice how the n^+p cell shows a significant radiation resistance over both the p^+n DJ cell as well as the GaAs/Ge cell. From this plot can be assumed a more beneficial design for multijunction cells composed of InGaP on top of GaAs with the n^+p design junction.

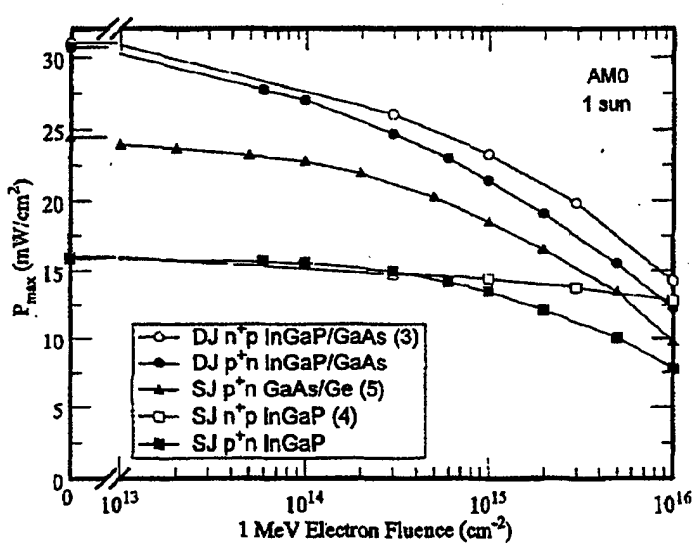

Figure 18. Comparison of response of SJ and DJ p^+n InGaP/GaAs cells with SJ and DJ n^+p InGaP/GaAs and SJ GaAs/Ge [Ref. 13]

C. THE CASE FOR COMPUTER MODELS IN SUPPORT OF MULTIJUNCTION CELL DEVELOPMENT

The design of the Spectrolab dual junction cell illustrates a reason for use of a computer model in development of advanced solar cells (and most semiconductor devices in general). Having a computer-modeling tool available to try what if type ideas, adjusting the many variables involved and finding just the right values to achieve your goals is much less expensive in terms of time and money than actually fabricating a cell and testing it. The model developed in this thesis is intended to closely duplicate the characteristics (or possible characteristics) of this jointly developed cell. The author's ideal hope would be that such a model would be of assistance to someone seeking to further advance the technology involved while producing an even more advanced cell.

D. DUAL JUNCTION BASELINE CELL TO MODEL

The materials chosen for the active layers of the Spectrolab cell were Gallium Indium Phosphide ($GaInP_2$) for the top cell, Gallium Arsenide (GaAs) for the middle cell, and Germanium (Ge) for the substrate. As shown in the figure 19, the dual junction cell is basically a building block for the triple junction cell shown in figure 20. By the addition of an Aluminum Gallium Arsenide window layer and a p Ge portion of the substrate, the dual junction cell becomes a triple junction cell.

Proprietary details concerning the design and manufacture of the dual junction cell from the ManTech program are not available to the author. This is not a complete hindrance. From the literature, many of the required parameters can be drawn and educated assumptions made. As mentioned in the introduction to this thesis, the main

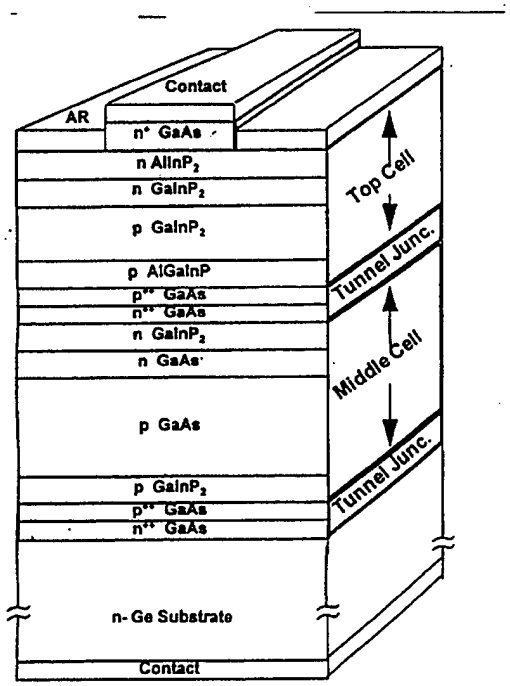

Figure 19. Dual Junction Cell Developed by Spectrolab for ManTech Program [Ref. 14]

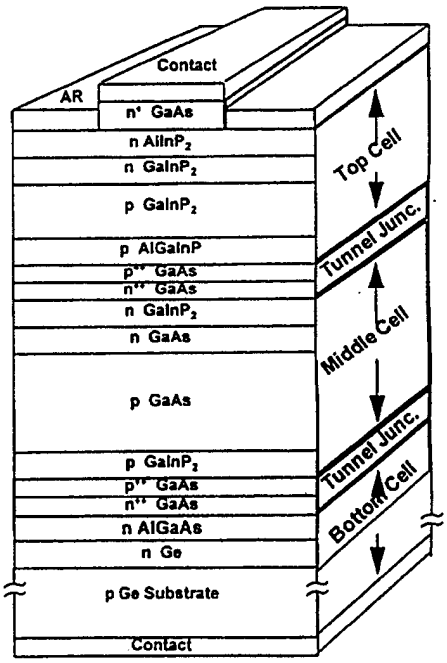

Figure 20. Triple Junction Cell Developed by Spectrolab for ManTech Program [Ref. 14]

goal is to build a model that is easily scaled and modified. While exact details would have made the work a little less time consuming, the desire to choose a cell design that is as close to state of the art as possible over-ruled. The added benefit of this cell is that it will indubitably be a starting point for future development and increased research.

1. Materials Selected for the Dual Junction Cell

There is a great deal of reference in the literature to AlGaAs as a photovoltaic material. A material of focus that exhibits a similar bandgap is $GaInP_2$. While details concerning the manufacturing process and specifics of this cell are proprietary and not available to the author, it can be inferred from the literature why $GaInP_2$ is used.

AlGaAs is susceptible to O_2 and H_2O that are unavoidably in the background during the Metalorganic Chemical Vapor Deposition (MOCVD) process. $GaInP_2$ is relatively insensitive to the levels of these two pollutants experienced during MOCVD and is also not affected by the extreme conditions required to grow the high conductance GaAs tunnel diode cell interconnects [Ref. 15].

A brief discussion of radiation testing and classification is required at this point for the reader who may not be familiar with this procedure and the accepted standards. Several facilities exist in the United States and other countries to subject various materials to radiation doses for the purpose of determining survivability in various environments. Radiation doses are administered and measured in fluences. 1 MeV electrons is a common dose for comparisons. Protons can also be administered.

Single layer silicon cells have one pn junction. As discussed earlier, this junction comes about by doping a previously p or n doped wafer with a material that will result in

either an n or p doped shallow layer at the top surface. Such a silicon cell typically displays an efficiency of approximately 15%.

As shown earlier, a single cell has a specific reaction to a given section of the solar spectrum. Different materials react to different segments of the solar spectrum based on the bandgap energy of the electrons in the valence band of the atoms. Figure 21 illustrates how the subsequent layers in a multijunction cell are optimized to ever increasing wavelengths of light. By bringing together the advantages of individual cells we can combine the strengths of those cells into a "stacked" cell. By building a cell composed of layers of varying materials we take advantage of these differences and

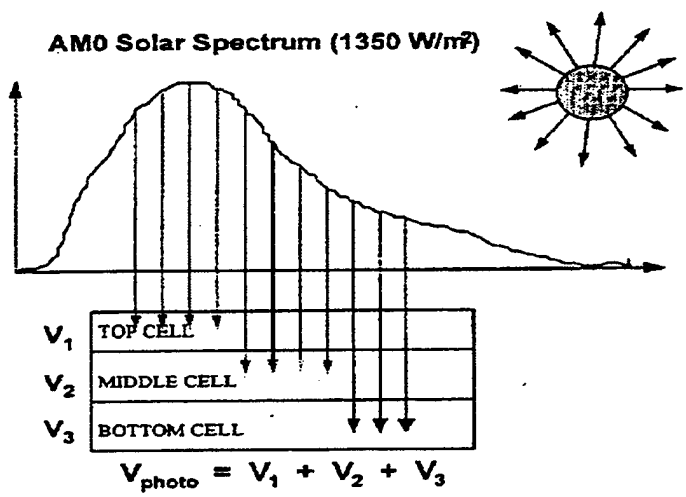

Figure 21. Each subcell in a MJ solar cell converts a specific range of wavelengths [Ref. 1]

produce a solar cell with a higher total efficiency than any one of the individual layers. In the Spectrolab cell the top cell consists of GaInP2, which has bandgap energy of 1.749 eV. (This value was determined using equation 5 below.) The middle cell consists of

GaAs, which has bandgap energy of 1.42 eV [Ref. 3]. The triple junction cell has a bottom cell made of Ge, which has bandgap energy of 0.66 eV [Ref. 3].

$$E_G(Ga_x In_{1-x} P) = 1.34 + 0.511x + 0.6043x^2 \qquad (5)$$

Equation 5 is the compositional dependence of the energy gap in III-V ternary alloy semiconductors at 300° K [Ref. 15].

Several challenges face the developer of a multi-junction solar cell. Selection of basic active layer materials, window layers, anti-reflection coatings, ohmic contact materials, tunnel junction construction, and current matching are but a few of the considerations facing the multijunction cell designer.

Tunnel diodes present a difficult challenge in the modeling of this cell. In order to take advantage of the current produced by the individual active junction layers, that current must be allow to conduct from the top of the cell to the bottom. Somehow, a contact must be made between each active layer that is made of a conducting material that is also transparent to the wavelengths of light that are intended for the next deeper active layer.

As with the InP related materials chosen for the active layers, a great deal of research and progress in the area of tunnel junction technology is reported in the literature. The issue is how to ensure the free electron hole pairs formed when incident photons break electrons loose from their valence band positions are not blocked from moving toward the eventual electrodes that ensure current flows. Tunnel junctions are the subjects of great research. The designers of the ManTech DJ cell used GaAs in a p++

on n++ configuration to ensure the flow would be one way and that the bandgap would be sufficiently wide to allow the light from above to continue to pass through as uninterrupted as possible. The reader is referred to Reference 16 for further information concerning tunnel diodes and interconnects in multijunction solar cells.

Window layers are required to reduce surface recombination of carriers. By inducing an energy discontinuity at the heterojunction of window layer material and active photovoltaic layer material, a minority carrier mirror is produced [Ref. 17]. Figure 22 shows the energy discontinuity in an $In_{0.52}Al_{0.48}As$ window layer on an InP (n^+p) active photovoltaic layer. Like the tunnel diode layers, the window layers were chosen and engineered to ensure the same results, maximal passage of incident light photons while ensuring minimal interference with "migrating" electrons and holes.

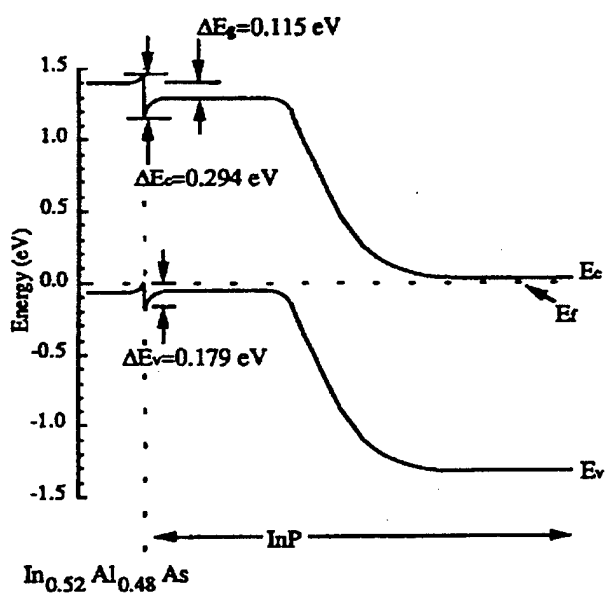

Figure 22. Energy band diagram of a p^+ InAlAs window layer on an InP Solar Cell [Ref. 17]

THIS PAGE INTENTIONALLY LEFT BLANK

V. CONCLUSIONS AND RECOMMENDATIONS

The overall goal of this effort is to develop a model of multijunction solar cells that is accurate and can be tailored to include various designs and variations as well as future incarnations and improvements. What was involved in developing that model to this point has been a large quantity of research and trial and error. In many ways, the trial and error is similar to what may be experienced by solar cell developers who manufacture a specific cell design on a test wafer fabrication facility in order to just test certain aspects of their design. The Silvaco Inc semiconductor device simulator allows that same trial and error approach with a very significant cost difference. To develop, manufacture and test a new cell design (however slightly modified from previous incarnations) in Silvaco costs nothing more than the time to input the new parameters and run the simulation. While the simulations can sometimes take hours (in most cases minutes) the time saved alone can be measured in weeks and months. Fabrication of a test solar cell on a wafer will take as much as weeks and can be extremely expensive on a small capacity project like research and development.

With the possibility of such vast savings for the industry in mind, the author set out to develop a model that was scalable and flexible, yet complex enough to handle the wide range of materials and parameters involved in semiconductor device design, fabrication, and testing. What follows is the collection of both the vision of what can be as well as the results of what was achieved to this point. While it will be seen that the ultimate goal of a workable model has yet to be achieved, many successes have laid the groundwork to achieving that goal.

A. CONCLUSIONS

Some difficulties arose as the author built the models for the multijunction cell. A workable solution is available for each of these stumbling points and generally a more thorough knowledge of the Silvaco software product proved sufficient to overcome them. The conclusion being that the desired model can be built. A model that builds the entire multiple layered, dual junction solar cell as illustrated in previous Chapters is included in Appendix B. Several portions of the model are also available. The individual portions are designed to focus on specific characteristics of individual layers. The vast array of capabilities exists within the Silvaco suite of simulation products.

In order to utilize the Silvaco family of semiconductor device simulators a UNIX computer network system is required. While Silvaco support's a PC version of some of the capabilities resident in the full UNIX version, it is limited in its scope by the unavailability of all packages. Primarily, the PC based packages available from Silvaco are intended as viewers for data and graphics produced with the more robust and complete UNIX based systems.

Silvaco supports a wide range of semiconductors, both single element and various compound materials. By paying close attention to the manuals, it is noticed that not every package within the Silvaco product supports all of the wide range of materials. Silicon is universally available but GaInP and GaAs were not recognized by all of them. In DECKBUILD, the pull-down menus list both GaAs and GaInP as choices in constructing a device. A problem arises when importing the DECKBUILD device into ATLAS. It is sometimes necessary to designate a region as one material that is more

widely supported and then change that region to the intended material later with ATHENA for example.

1. Assumptions

First, some assumptions and simplifications were made during the development of the model of the dual junction cell. Uniform doping was employed. In reality, each material would have been laid down as a new layer in a process such as MOCVD or Molecular Beam Epitaxy (MBE) and then the pn junction would be formed by diffusing a dopant into the top surface of the specific material. Following that, the next major material would be laid down and the junction formed again by diffusion. This would have been repeated until the entire cell was formed. By just inputting uniform doping, the cell was instantaneously assembled, bypassing the Virtual Wafer Fabrication facility resident in Silvaco. More accurate models will eventually need to take into account the growth procedures intended for actual wafer fabrication.

2. Silicon Model Variations

For comparison's sake, several models were run for a simple Silicon solar cell. The solar cell model included with Silvaco was used as the baseline for this model with only slight modifications. Many thanks to the individuals at Silvaco who assisted via e-mail. The modified model input code and the resulting I/V curves are included in appendix A. For the simple silicon cell, variables were modified in order to show the effects on the resulting I/V curves. The doping, cell thickness, doping materials, and cell

geometry (anode size), were all modified in order to show the results. Also apparent from observing these results are some limitations of the Silvaco model for solar cells as we are simulating them.

Doping was modified both up and down and the polarity of the cell was reversed (np and pn) in order to illustrate the effects and gain confidence in the model. The doping will effect the basic characteristics of the pn junction. The doping would also effect the carrier lifetime and diffusion lengths, both effecting the total current realized from the cell. In the cases where these parameters were modified and run, the results generally agree with theory and experience.

Cell thickness was increased and decreased. The expected results in the increased thickness case would be less current "collection" due to more electron hole pair recombination. The total effect this would have on current at the cathode would be determined by diffusion length and carrier lifetime.

The doping materials used were modified and the results also included in Appendix A. The effect was not expected to be great. Silvaco has within its command capabilities the ability to add generic "n" and "p" doping, requiring no particular need to identify a specific dopant.

The cell geometry modified in this case refers to the size of the aluminum contact material on the top surface of the cell. As described earlier, the contacts necessarily should cover as little surface area as possible in order to shade the cell minimally, while still providing sufficient coverage to collect current before the electron hole pairs recombine. The width of the contacts is also controlled by the particular manufacturing

technology employed by the cell manufacturer in that they cannot be narrower than the current process technology and lithography allows.

In addition to the basic silicon models, more advanced III-V material models were developed. Again, the basic model of a silicon cell was used as a baseline but obviously many more changes were made in the process of developing a III-V material model. The basic geometry of a GaAs active layer cell on a Ge substrate (omitting the GaAs tunnel diode layer) was taken from the crude diagram provided from Phillips Research Lab in Kirtland AFB, NM. This diagram, shown in Figure 19 in Chapter IV, does not include the dimensions of the individual layers. Thickness' used in the models developed here were taken a paper by Lammasniemi et al. (shown in Figure 23) that discussed a cell grown by MBE at the Tampere University of Technology in Finland [Ref. 18]. This MBE grown cell demonstrated 21.1% efficiency under AM0 conditions. The arrangement and materials of the basic cell layers were very similar to the cell diagram provided by Phillips Lab (Figure 19).

The input code and Silvaco produced device structure plots for the dual junction cell illustrated in figures 19 and 23 are included in Appendix B. The input code and device structure plot for the single junction GaAs cell on Ge substrate are included in Appendix C.

B. RECOMMENDATIONS

Several avenues exist for future work. Future work on this project should first focus on improving the accuracy of the models produced thus far. The addition of another pn junction layer to the existing model would carry this work to the next level already under

consideration in the industry [Ref. 1]. Simulation of radiation damage and annealing effects could also be pursued. The cells provided by the Program Manager of the joint project at Phillips Labs are also still available to provide experimental data for comparisons to model outputs.

Whatever area the future student may wish to work on, it is highly recommended that the student first become familiar with the Silvaco product. Working with the students in the VLSI laboratory proved highly helpful in this regard.

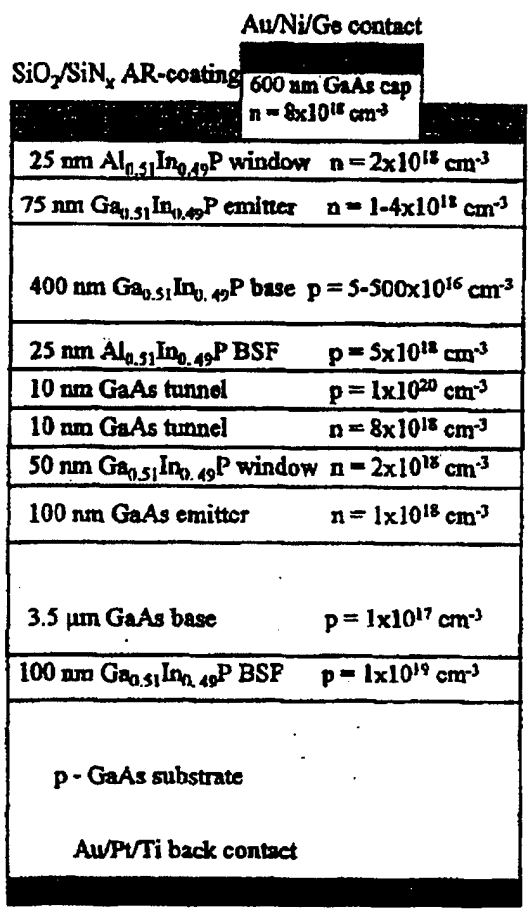

Figure 23. A Dual Junction Solar Cell Grown by MBE [Ref. 17]

APPENDIX A. INPUT CODE FOR SINGLE JUNCTION SILICON CELL

The following is the input code for a single junction silicon solar cell. The basic design is from the Silvaco example file optoex08.in that is provided under the main control pull-down menu in DECKBUILD. The main modification is the addition of a rampdown.log file that saves data from the stepped bias voltage. The lines

```
#switch cathode back to voltage control
contact name=cathode ^current
#open logfile for ramp
log outf=rampdown.log
#ramp vcathode from Open circuit value to zero
solve prev b1=1
solve vstep=0.1 vfinal=0.1 name=cathode b1=1
solve vcathode=0 b1=1
```

first switch the cathode back to voltage controlled and then step the cathode external bias from the previously extracted open circuit voltage down to zero (or in this case 0.1V).

```
#File for plotting I/V curve of basic Si cell example
#tonyplot must be modified to display cathode current against cath bias
#12:42, 8 July 99
#Darin McCloy
#modified 12 July to see what happens when .set files are not ref'd for tonyplot
#results show a flipped I/V curve with negative current values
#structure file tonyplot view shows only material make-up not photogeneration
#rates
#31 aug modified Si doping to 1e16 boron vice 1e14 and mod phos dop to 1e16
vice
#1e15 to see what effect it has on I/V curve (.4 volts before)
go athena
#
line x loc=0.00 spac=1
line x loc=10 spac=1
#
line y loc=0.00 spac=0.05
line y loc=0.25 spac=0.02
line y loc=1 spac=0.1
```

```
line y loc=50 spac=10
init silicon c.boron=1.0e16 orientation=100
# deposit oxide coating
deposit oxide thickness=0.05
# implant n+ layer
implant phos dose=1e16 energy=30
# drive-in
diffuse time=10 temp=900
# extract n layer junction depth
extract name="junc_depth" xj material="Silicon" mat.occno=1 x.val=0.1
junc.occno=1
# form contact
etch oxide right p1.x=8
deposit alum thickness=0.1 div=3
etch alum left p1.x=8
# relax the mesh in deep area
relax y.min=0.6
relax y.min=2.0
relax y.min=10
# Reflect to get complete structure
structure mirror right
# set electrodes for ATLAS
electrode name=cathode x=10
electrode name=anode backside
structure outf=optoex08_0.str
go atlas
# set contact material to be opaque
material material=Aluminum imag.index=1000
material material=Silicon  taun0=1e-6 taup0=1e-6
# set light beam using solar spectrum from external file
beam  num=1 x.origin=10.0 y.origin=-2.0 angle=90.0 power.file=optoex08.spec
# saves optical intensity to solution files
output opt.int
models conmob fldmob srh print
# get open circuit voltage
solve init
contact name=cathode current
log outf=ocv.log
solve icathode=0 b1=1
#test input
#end
#quit
#test input
extract name="open_circuit_voltage" max(abs(vint."cathode"))
#switch cathode back to voltage control
```

```
contact name=cathode ^current
#open logfile for ramp
log outf=rampdown.log
#ramp vcathode from Open circuit value to zero
solve prev b1=1
solve vstep=0.1 vfinal=0.1 name=cathode b1=1
solve vcathode=0 b1=1
extract name="short_circuit_current" max(abs(i."cathode"))
save outf=optoex08_2.str
tonyplot optoex08_2.str
#remove comments and move next line back to end of previous line
#-set optoex08_2.set
go atlas
#
# SECOND ATLAS RUN FOR SPECTRAL RESPONSE
# set contact material to be opaque
material material=Aluminum imag.index=1000
material material=Silicon  taun0=1e-6 taup0=1e-6
# set monochromatic light beam for spectral analysis
beam  num=1 x.origin=10.0 y.origin=-2.0 angle=90.0
# saves optical intensity to solution files
output opt.int
models conmob fldmob srh print
# spectral response
solve init b1=.1
log outf=optoex08_2.log
solve b1=1 lambda=0.3
solve b1=1 lambda=0.35
solve b1=1 lambda=0.4
solve b1=1 lambda=0.45
solve b1=1 lambda=0.5
solve b1=1 lambda=0.55
solve b1=1 lambda=0.6
solve b1=1 lambda=0.65
solve b1=1 lambda=0.7
solve b1=1 lambda=0.75
solve b1=1 lambda=0.8
solve b1=1 lambda=0.85
solve b1=1 lambda=0.9
solve b1=1 lambda=0.95
solve b1=1 lambda=1.00
tonyplot rampdown.log
#remove comments and move next line to end of previous line
#-set optoex08_3.set
quit
```

I/V CURVE OF SILICON SOLAR CELL

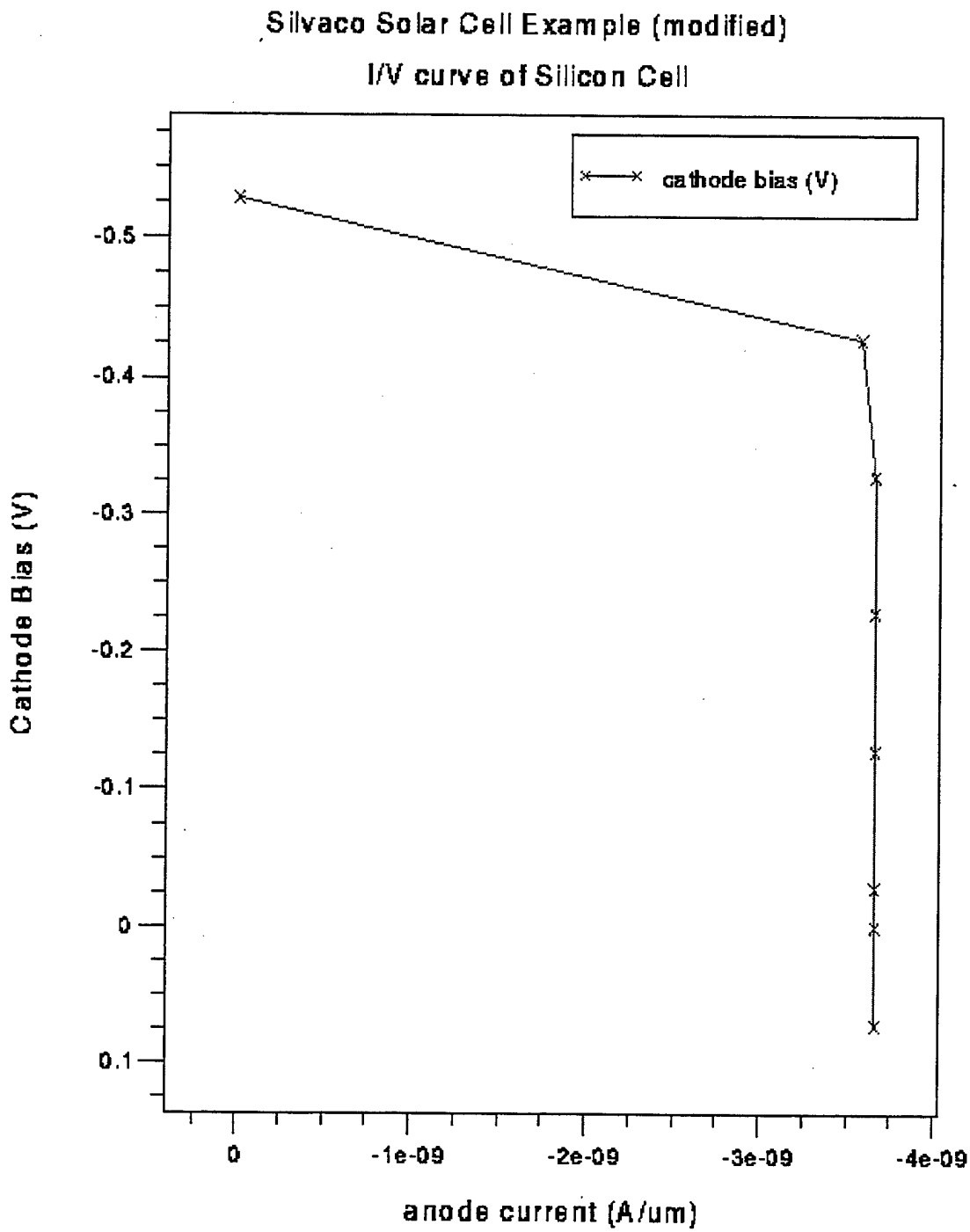

APPENDIX B. INPUT CODE FOR DUAL JUNCTION CELL

The following is the input code for the model of the dual junction cell. This code can be input directly into the file-input screen of DECKBUILD. Certain modifications were made to this model setup in order to use Silvaco specified materials. Notes in the first two lines were made by the author in order to keep track of versions and cue the user to the cell modeled in each set of instructions. Notice the first non-commented line of text, "go devedit". This and the following line indicating the version of DEVEDIT used are required when importing a structure/device drawn in DEVEDIT and then modeled in DECKBUILD. To design a cell in this manner simply draw the cell (or any device) in DEVEDIT. Once the device is complete, save the file as "commands", one of the choices in the save dialog box. Be sure to append the .in suffix to the filename. Then open DECKBUILD and load the previously constructed file that was just saved as "commands". The commands that specify the structure of the previous drawn device are automatically converted to text based input code as seen in the following pages. The two lines specified above, "go devedit", and "devedit version X.XX" are added by the user. At the end of the automatically generated code the user then specifies either ATLAS or ATHENA to continue performing the simulation. See the Silvaco User's Manuals for further details [ATLAS manual].

```
#5 Sept 99
#full cell (dual junction solar cell)
#
go devedit
DevEdit version=2.4.0.R
work.area x1=0 y1=-0.1 x2=20 y2=20
# devedit 2.4.0.R (Thu May  8 12:10:49 PDT 1997)
# libsflm 2.0.0.R (Thu May  1 19:30:21 PDT 1997)
```

```
# libDW_Misc 1.20.0.R (Tue Apr 29 01:46:55 PDT 1997)
# libCardDeck 1.20.0.R (Tue Apr 29 14:47:22 PDT 1997)
# libGeometry 1.20.0.R (Tue Apr 29 02:15:40 PDT 1997)
# libDW_Set 1.20.0.R (Tue Apr 29 01:48:02 PDT 1997)
# libSVC_Misc 1.20.0.R (Tue Apr 29 02:17:47 PDT 1997)
# libSDB 1.0.6.C (Mon May  5 16:30:46 PDT 1997)
# libSSS 1.20.0.R (Mon May  5 16:31:52 PDT 1997)
# libMeshBuild 1.20.0.R (Thu May  8 00:04:50 PDT 1997)
# libDW_Make 1.1.3.R (Thu May  1 20:07:42 PDT 1997)
region reg=1 name=anode mat=Aluminum elec.id=1 work.func=0 \
        polygon="12,-0.1 12,0 8,0 8,-0.1"
#
constr.mesh region=1 default
region reg=2 mat=GaAs \
        polygon="12,0.2 12,0.6 8,0.6 8,0.2 8,0 12,0"
#
constr.mesh region=2 default
region reg=3 mat=SiN \
        polygon="8,0.2 8,0.6 0,0.6 0,0.2"
#
constr.mesh region=3 default
region reg=4 mat=SiN \
        polygon="20,0.2 20,0.6 12,0.6 12,0.2"
#
constr.mesh region=4 default
region reg=5 name="window (p)" mat=InAlAs \
        polygon="20,0.6 20,0.625 0,0.625 0,0.6 8,0.6 12,0.6"
#
constr.mesh region=5 default
region reg=6 name=emitter mat=InGaP \
        polygon="20,0.625 20,0.7 0,0.7 0,0.625"
#
constr.mesh region=6 default
region reg=7 mat=InGaP \
        polygon="20,0.7 20,1.1 0,1.1 0,0.7"
#
constr.mesh region=7 default
region reg=8 mat=InAlAs \
        polygon="20,1.1 20,1.125 0,1.125 0,1.1"
#
constr.mesh region=8 default
region reg=9 name="tunnel diode" mat=GaAs \
        polygon="20,1.125 20,1.135 0,1.135 0,1.125"
#
constr.mesh region=9 default
```

```
region reg=10 mat=GaAs \
        polygon="20,1.135 20,1.145 0,1.145 0,1.135"
#
constr.mesh region=10 default
region reg=11 name=window mat=InGaP \
        polygon="20,1.145 20,1.195 0,1.195 0,1.145"
#
constr.mesh region=11 default
region reg=12 name=emitter mat=GaAs \
        polygon="20,1.195 20,1.295 0,1.295 0,1.195"
#
constr.mesh region=12 default
region reg=13 name=base mat=GaAs \
        polygon="0,4.795 0,1.295 20,1.295 20,4.795"
#
constr.mesh region=13 default
region reg=14 name=BSF mat=InGaP \
        polygon="20,4.795 20,4.895 0,4.895 0,4.795"
#
constr.mesh region=14 default
region reg=15 name="tunnel (p++)" mat=GaAs \
        polygon="20,4.895 20,4.905 0,4.905 0,4.895"
#
constr.mesh region=15 default
region reg=16 name="tunnel (n++)" mat=GaAs \
        polygon="20,4.905 20,4.915 0,4.915 0,4.905"
#
constr.mesh region=16 default
region reg=17 name=cathode mat=Aluminum elec.id=2 work.func=0 \
        polygon="20,19.9 20,20 0,20 0,19.9"
#
constr.mesh region=17 default
region reg=18 name="Substrate (n)" mat=Germanium \
        polygon="0,19.9 0,4.915 20,4.915 20,19.9"
#
constr.mesh region=18 default
# Set Meshing Parameters
#
base.mesh height=10 width=10
#
bound.cond !apply max.slope=30 max.ratio=100 rnd.unit=0.001
line.straightening=1 align.points when=automatic
#
imp.refine min.spacing=0.02
#
```

```
constr.mesh  max.angle=90 max.ratio=300 max.height=10000 \
        max.width=10000 min.height=0.0001 min.width=0.0001
#
constr.mesh type=Semiconductor default
#
constr.mesh type=Insulator default
#
constr.mesh type=Metal default
#
constr.mesh type=Other default
#
constr.mesh region=1 default
#
constr.mesh region=2 default
#
constr.mesh region=3 default
#
constr.mesh region=4 default
#
constr.mesh region=5 default
#
constr.mesh region=6 default
#
constr.mesh region=7 default
#
constr.mesh region=8 default
#
constr.mesh region=9 default
#
constr.mesh region=10 default
#
constr.mesh region=11 default
#
constr.mesh region=12 default
#
constr.mesh region=13 default
#
constr.mesh region=14 default
#
constr.mesh region=15 default
#
constr.mesh region=16 default
#
constr.mesh region=17 default
#
```

```
constr.mesh region=18 default
Mesh Mode=MeshBuild
refine mode=y x1=0.27 y1=1.55 x2=20.04 y2=5.12
refine mode=both x1=7.98 y1=-0.113 x2=12.19 y2=0.642
refine mode=both x1=-0.07 y1=0.09 x2=20.71 y2=5.98
base.mesh height=10 width=10
bound.cond !apply max.slope=30 max.ratio=100 rnd.unit=0.001
line.straightening=1 align.Points when=automatic
go atlas
structure outf=dualjun2_0.str
save outf=dualjun2_0.str
tonyplot dualjun2_0.str
# set contact material to be opaque
material material=Aluminum imag.index=1000
# set light beam using solar spectrum from external file
beam  num=1 x.origin=10.0 y.origin=-2.0 angle=90.0 power.file=optoex08.spec
# saves optical intensity to solution files
output opt.int
models print conmob fldmob srh
# get open circuit voltage
solve init
contact name=cathode current
log outf=ocv.log
solve icathode=0 b1=1
#test input
#end
#quit
#test input
extract name="open_circuit_voltage" max(abs(vint."cathode"))
#switch cathode back to voltage control
contact name=cathode ^current
#open logfile for ramp
log outf=rampdown.log
#ramp vcathode from Open circuit value to zero
solve prev b1=1
solve vstep=0.1 vfinal=0.1 name=cathode b1=1
solve vcathode=0 b1=1
extract name="short_circuit_current" max(abs(i."cathode"))
save outf=dualjun2_1.str
tonyplot dualjun2_1.str
#remove comments and move next line back to end of previous line
#-set optoex08_2.set
go atlas
#
# SECOND ATLAS RUN FOR SPECTRAL RESPONSE
```

```
#
# set contact material to be opaque
material material=Aluminum imag.index=1000
material material=Silicon  taun0=1e-6 taup0=1e-6
# set monochromatic light beam for spectral analysis
beam  num=1 x.origin=10.0 y.origin=-2.0 angle=90.0
# saves optical intensity to solution files
output opt.int
models conmob fldmob srh print
# spectral response
solve init b1=.1
log outf=dualjun2_2.log
solve b1=1 lambda=0.3
solve b1=1 lambda=0.35
solve b1=1 lambda=0.4
solve b1=1 lambda=0.45
solve b1=1 lambda=0.5
solve b1=1 lambda=0.55
solve b1=1 lambda=0.6
solve b1=1 lambda=0.65
solve b1=1 lambda=0.7
solve b1=1 lambda=0.75
solve b1=1 lambda=0.8
solve b1=1 lambda=0.85
solve b1=1 lambda=0.9
solve b1=1 lambda=0.95
solve b1=1 lambda=1.00
tonyplot rampdown.log
#remove comments and move next line to end of previous line
#-set optoex08_3.set
quit
```

Tonyplot presentation of the Dual Junction cell with layers indicated in various colors. The following pages show more detailed views of segments of this cell where individual layers are extremely thin and do not show up in this view.

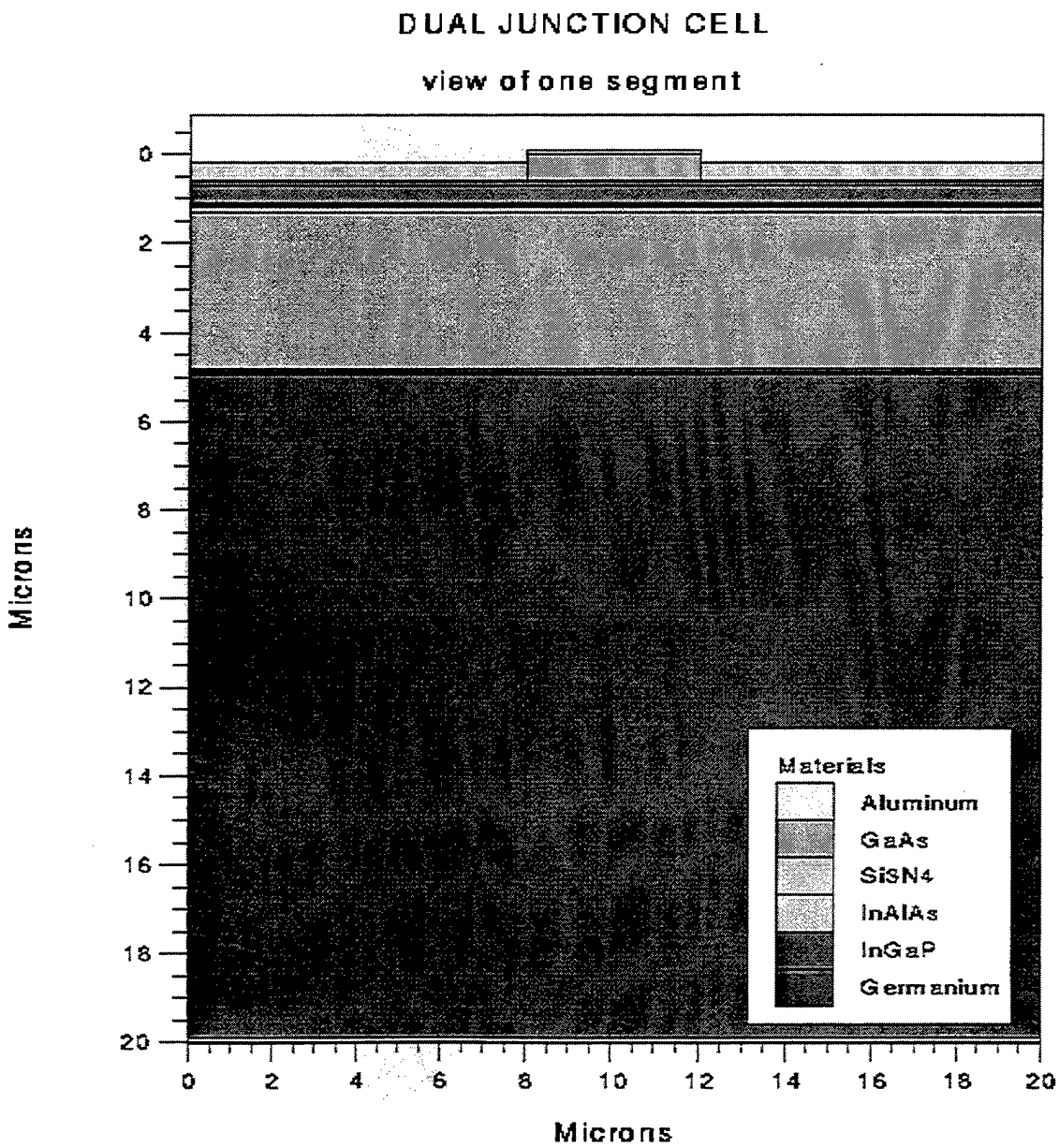

DUAL JUNCTION CELL

detail of layers near surface

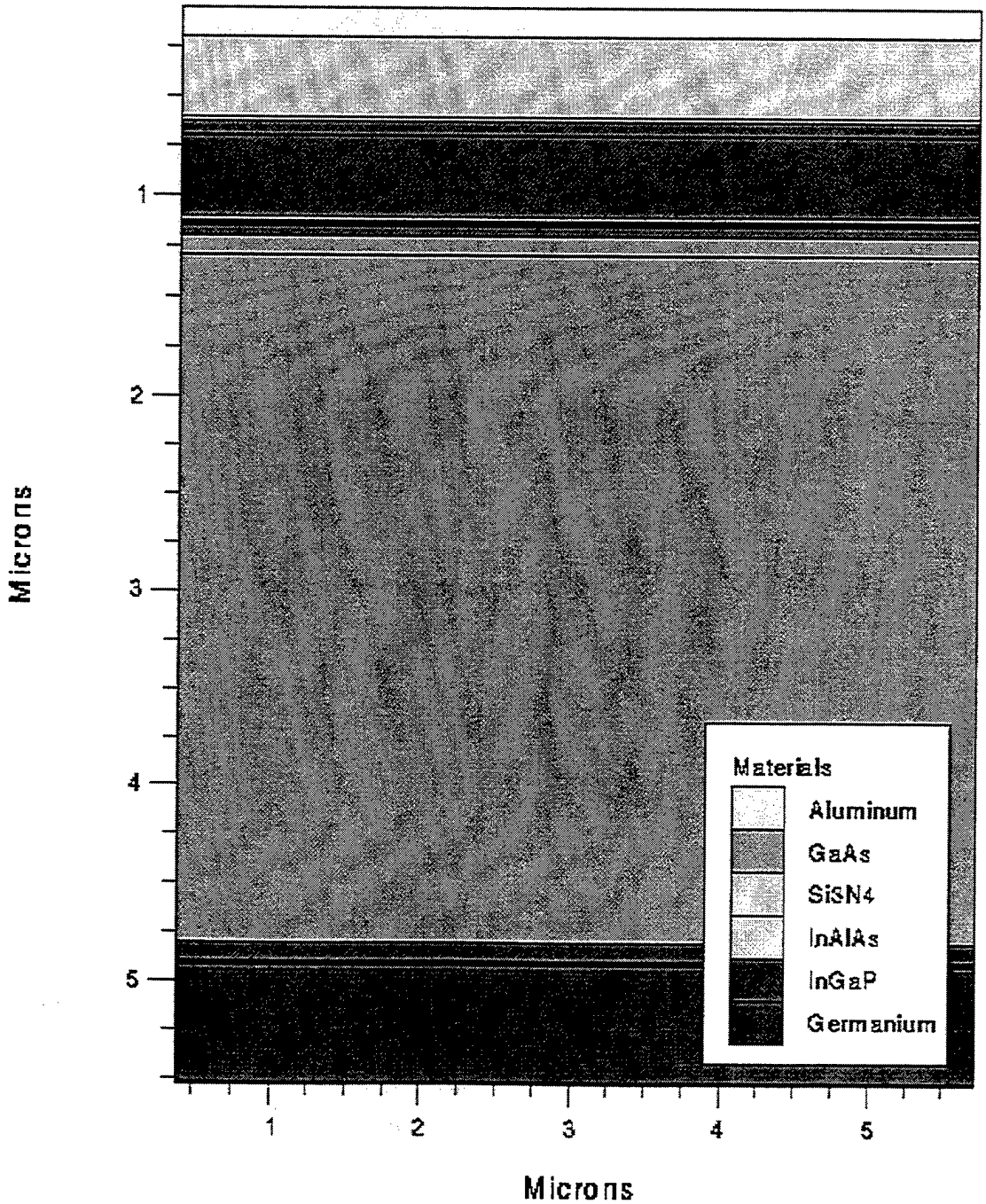

DUAL JUNCTION CELL

detail of 2nd window, GaAs tunnel and GaAs middle cell

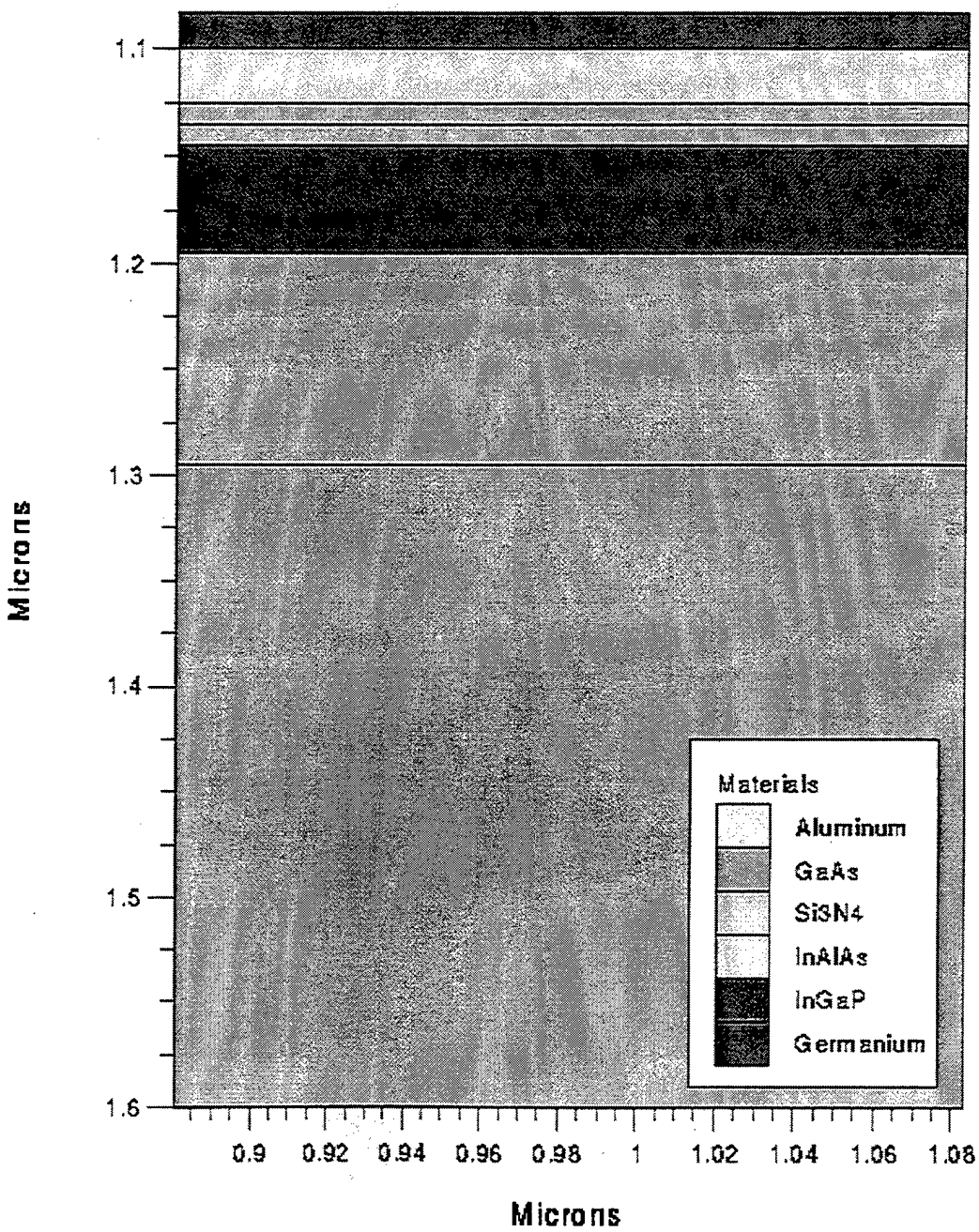

DUAL JUNCTION CELL

detail of middle cell BSF, 2nd GaAs tunnnel, and Ge substrate

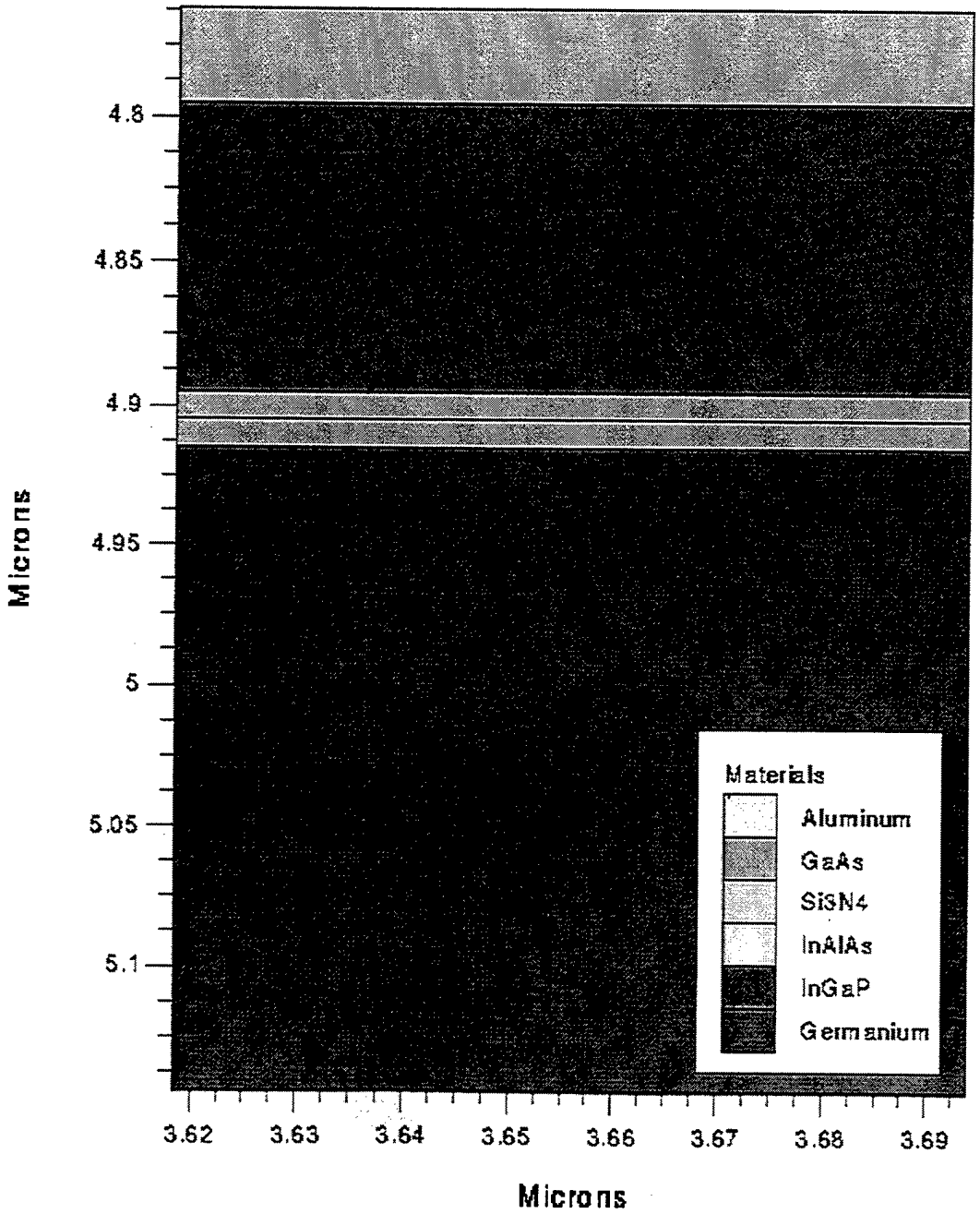

APPENDIX C. INPUT CODE FOR SINGLE JUNCTION GaAs CELL

The following code was developed to model a single junction GaAs solar cell on a germanium substrate. This was developed in a step by step manner as a building block/learning step toward reaching the eventual full Dual Junction cell.

```
#one cell, a GaAs active cell on germanium substrate
#16 Aug 99
#test steps added to run for output 20 Aug
#25 aug modified for detailed mesh in athena
#also doped to 1e18 p substr, 1e17 p base, 1e18 n emit
#31 aug changing substr doping to n-type
#also fixed doping statements
go devedit
DevEdit version=2.4.0.R
work.area x1=0 y1=-0.1 x2=20.0000009 y2=20.1
# devedit 2.4.0.R (Thu May  8 12:10:49 PDT 1997)
# libsflm 2.0.0.R (Thu May  1 19:30:21 PDT 1997)
# libDW_Misc 1.20.0.R (Tue Apr 29 01:46:55 PDT 1997)
# libCardDeck 1.20.0.R (Tue Apr 29 14:47:22 PDT 1997)
# libGeometry 1.20.0.R (Tue Apr 29 02:15:40 PDT 1997)
# libDW_Set 1.20.0.R (Tue Apr 29 01:48:02 PDT 1997)
# libSVC_Misc 1.20.0.R (Tue Apr 29 02:17:47 PDT 1997)
# libSDB 1.0.6.C (Mon May  5 16:30:46 PDT 1997)
# libSSS 1.20.0.R (Mon May  5 16:31:52 PDT 1997)
# libMeshBuild 1.20.0.R (Thu May  8 00:04:50 PDT 1997)
# libDW_Make 1.1.3.R (Thu May  1 20:07:42 PDT 1997)
region reg=1 name=substrate mat=Germanium color=0x8c8c8c pattern=0x1 \
        polygon="0,10 20,10 20,20 0,20"
#
constr.mesh region=1 default
region reg=2 name="base (GaAs)" mat=GaAs color=0x7f00 pattern=0x9 \
        polygon="0,6.5 20,6.5 20,10 0,10"
#
constr.mesh region=2 default
region reg=3 name="emitter (GaAs)" mat=GaAs color=0x7f00 pattern=0x9 \
        polygon="0,6.4 8,6.4 12,6.4 20,6.4 20,6.5 0,6.5"
#
constr.mesh region=3 default
region reg=4 name=cathode mat=Aluminum elec.id=1 work.func=0
color=0xffc8c8 pattern=0x7 \
```

```
        polygon="8,6.3 12,6.3 12,6.4 8,6.4"
#
constr.mesh region=4 default
region reg=5 name=anode mat=Aluminum elec.id=2 work.func=0 color=0xffc8c8
pattern=0x7 \
        polygon="0,20 20,20 20,20.1 0,20.1"
#
constr.mesh region=5 default
# Set Meshing Parameters
#
base.mesh height=10 width=10
#
bound.cond !apply max.slope=30 max.ratio=100 rnd.unit=0.001
line.straightening=1 align.points when=automatic
#
imp.refine min.spacing=0.02
#
constr.mesh  max.angle=90 max.ratio=300 max.height=10000 \
        max.width=10000 min.height=0.0001 min.width=0.0001
#
constr.mesh type=Semiconductor default
#
constr.mesh type=Insulator default
#
constr.mesh type=Metal default
#
constr.mesh type=Other default
#
constr.mesh region=1 default
#
constr.mesh region=2 default
#
constr.mesh region=3 default
#
constr.mesh region=4 default
#
constr.mesh region=5 default
Mesh Mode=MeshBuild
refine mode=both x1=-0.29 y1=5.82 x2=20.45 y2=20.75
refine mode=both x1=-0.14 y1=6.05 x2=20.27 y2=20.52
refine mode=both x1=-0.14 y1=5.97 x2=20.45 y2=20.56
refine mode=y x1=-0.005 y1=6.471 x2=2.036 y2=6.542
base.mesh height=10 width=10
bound.cond !apply max.slope=30 max.ratio=100 rnd.unit=0.001
line.straightening=1 align.Points when=automatic
```

```
go athena
#
line x loc=0.00 spac=1
line x loc=8 spac=0.2
line x loc=12 spac=1
line x loc=20 spac=1
#
line y loc=6.3 spac=0.05
line y loc=6.4 spac=0.02
line y loc=6.5 spac=0.001
line y loc=8 spac=0.05
line y loc=10 spac =0.001
line y loc=10.2 spac=0.05
line y loc=20 spac=0.01
line y loc=20.08 spac=0.01
#structure outf=onecell_1.str
go atlas
dop region=1 unif conc=1e18 n.type
dop region=2 unif conc=1e17 p.type
dop region=3 unif conc=1e18 n.type
# vtonyplot onecell_1.str
# set contact material to be opaque
material material=Aluminum imag.index=1000
#material material=Silicon  taun0=1e-6 taup0=1e-6
# set light beam using solar spectrum from external file
beam  num=1 x.origin=10.0 y.origin=-2.0 angle=90.0 power.file=optoex08.spec
# saves optical intensity to solution files
output opt.int

models conmob fldmob srh print
# get open circuit voltage
solve init
contact name=cathode current
log outf=ocv.log
solve icathode=0 b1=1
#test input
#end
#quit
#test input
extract name="open_circuit_voltage" max(abs(vint."cathode"))
#switch cathode back to voltage control
contact name=cathode ^current
#save outf=onecell2_2.str
#tonyplot onecell2_2.str
#-set optoex08_2.set
```

```
#open logfile for ramp
log outf=rampdown2.log
#ramp vcathode from Open circuit value to zero
solve prev b1=1
solve vstep=0.1 vfinal=0.1 name=cathode b1=1
solve vcathode=0 b1=1
extract name="short_circuit_current" max(abs(i."cathode"))
save outf=onecell_2.str
tonyplot onecell_2.str
#remove comments and move next line back to end of previous line
#-set optoex08_2.set
go atlas
#
# SECOND ATLAS RUN FOR SPECTRAL RESPONSE
#
# set contact material to be opaque
material material=Aluminum imag.index=1000
# set monochromatic light beam for spectral analysis
beam  num=1 x.origin=10.0 y.origin=-2.0 angle=90.0
# saves optical intensity to solution files
output opt.int
models conmob fldmob srh print
# spectral response
solve init b1=.1
log outf=onecell_2.log
solve b1=1 lambda=0.3
solve b1=1 lambda=0.35
solve b1=1 lambda=0.4
solve b1=1 lambda=0.45
solve b1=1 lambda=0.5
solve b1=1 lambda=0.55
solve b1=1 lambda=0.6
solve b1=1 lambda=0.65
solve b1=1 lambda=0.7
solve b1=1 lambda=0.75
solve b1=1 lambda=0.8
solve b1=1 lambda=0.85
solve b1=1 lambda=0.9
solve b1=1 lambda=0.95
solve b1=1 lambda=1.00
tonyplot rampdown2.log
#-set optoex08_3.set
quit
```

Tonyplot presentation of the Single Junction GaAs/Ge cell with layers indicated in various colors.

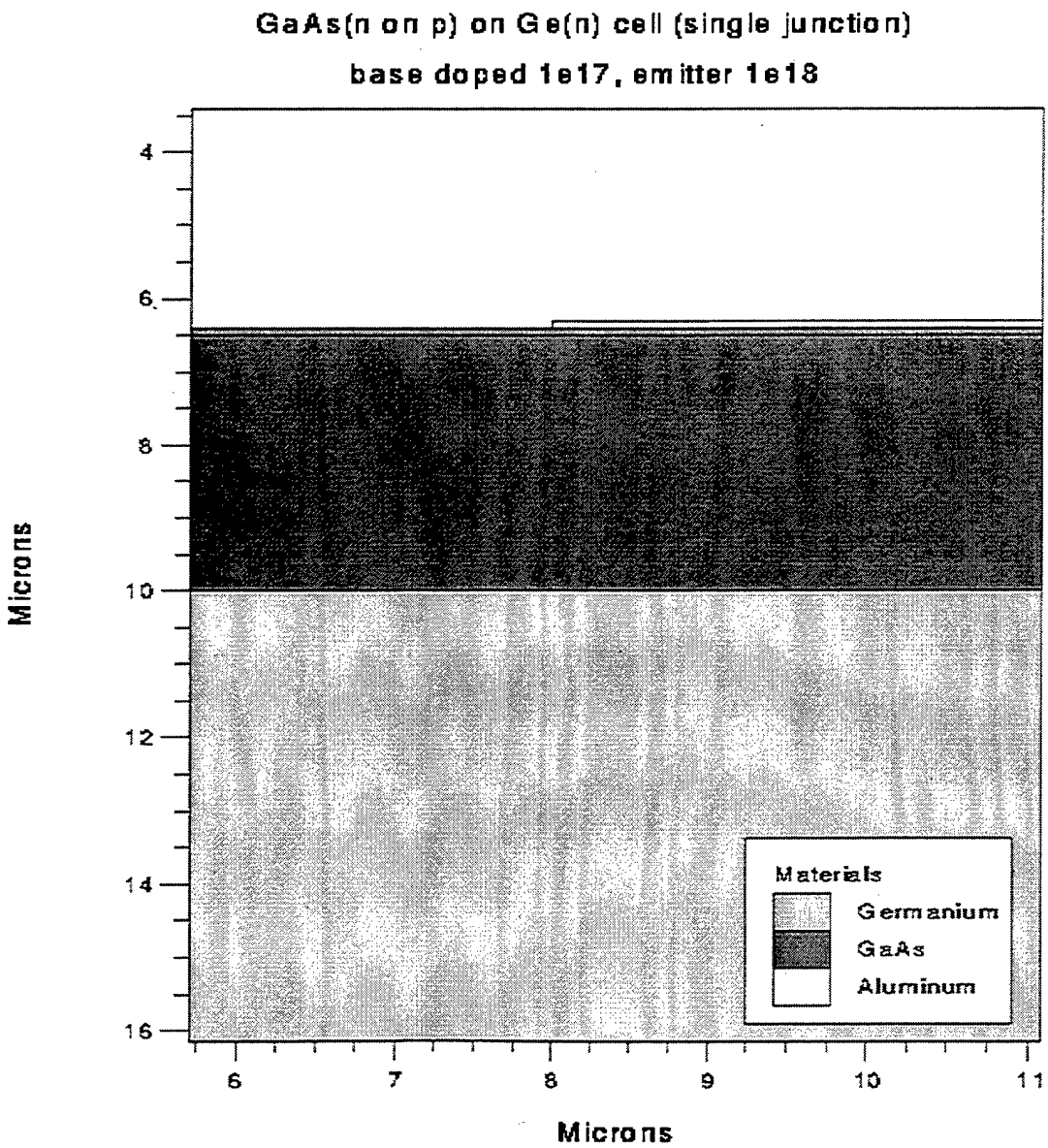

THIS PAGE INTENTIONALLY LEFT BLANK

LIST OF REFERENCES

1. D.N. Keener, D.C. Marvin, D.J. Brinker, H.B. Curtis, P.M. Price, "Progress Toward Technology Transition of $GaInP_2$/GaAs/Ge Multijunction Solar Cells", *Proc. 26th IEEE Photovoltaic Specialists Conference*, 29 Sept.-3 Oct. 1997.

2. Chemical Societies Network, The, "The Visual Elements Periodic Table," [http://www.chemsoc.org/viselements/pages/periodic_table.html]

3. Robert F. Pierret, *Semiconductor Device Fundamentals*, Addison Wesley, 1996.

4. Lynn Boyer, *Power Recovery of radiation Damaged MOCVD Grown Indium Phosphide on Silicon Solar Cells Through Argon-Ion Laser Annealing*, Masters Thesis, Naval Postgraduate School, Monterey, CA, 1996.

5. Michael Shur, *Physics of Semiconductor Devices*, Prentice Hall, 1990.

6. Kevin F. Brennan, *The Physics of Semiconductors, With Applications to Optoelectronic Devices*, Cambridge University Press, 1999.

7. Sherif Michael, "Space Power and Radiation Effects," Naval Postgraduate School Class Notes for EC3230, 1994 (unpublished).

8. J. Sutherland, "A Computer Analysis of Heterojunction and Graded Composition Solar Cells," *IEEE Transactions on Electron Devices*, Vol ED-24, No. 4, April 1977.

9. Silvaco International, *ATLAS User's Manual, Device Simulation Software*, Version 4.0, 1995.

10. http://www.silvaco.com/applications/hints/jun95_1/fig3.gif)

11. E.L. Ralph, "High Efficiency Solar Cell Arrays System Trade-offs," *Proc. 24th IEEE Photovoltaic Specialists Conference*, 5-9 Dec, 1994.

12. E.B. Linder, J.P. Hanley, "Manufacturing Experience with GaInP2/GaAs/Ge Solar Panels for Space Demonstration," *Proc. of 25th Photvoltaic Specialists Conference*, May 13-17, 1996, Washington, D.C.

13. R.J. Walters, M.A. Xapsos, and G.P. Summers, "Radiation Response of Single and Dual Junction p^+n InGaP/GaAs Space Cells," *26th IEEE Photvoltaic Specialists Conference*, 30 Sept-3 Oct, 1997, Anaheim, CA.

14. Spectrolab, Inc, "$GaInP_2$/GaAs/Ge Baseline Demonstration Cell Cross Sections," unpublished, undated.

15. Avishay Katz, editor, *Indium Phosphide and Related Materials: Processing, Technology, and Devices*, Artech House, 1992.

16. J.M. Olson, S.R. Kurtz, A.E. Kibler, "A 21.8% $GaInP_2$/GaAs Tandem Solar Cell," *Proc. 20th IEEE Photovoltaic Specialists Conference*, 26-30 Sept., 1988

17. R.K. Jain, G.A. Landis, D.J. Flood, "Lattice Matched $In_{0.52}Al_{0.48}As$ Window Layers for InP Solar Cells," *Proc. Fourth International Conference on Indium Phosphide Related Materials*, 21-24 April, 1992.

18. Lammasniemi, J.; Tappura, K.; Jaakkola, R.; Kazantsev, A.; Rakennus, K.; Uusimaa, P.; Pessa, M., "Molecular Beam Epitaxy Grown GaInP Top Cells and GaAs Tunnel Diodes for Tandem Applications," *Proc. 25th, IEEE Photovoltaic Specialists Conference*, 13-17 May 1996, Washington, D.C.

INITIAL DISTRIBUTION LIST

1. Defense Technical Information Center.....2
   8725 John J. Kingman Rd., STE 0944
   Ft. Belvoir, Virginia 22060-6218

2. Dudley Knox Library.....2
   Naval Postgraduate School
   411 Dyer Rd.
   Monterey, California 93943-5101

3. Director, Training and Education.....1
   MCCDC, Code C46
   1019 Elliot Rd.
   Quantico, Virginia 22134-5107

4. Director, Marine Corps Research Center.....2
   MCCDC, Code C40RC
   2040 Broadway Street
   Quantico, Virginia 22134-5107

5. Director, Studies and Analysis Division.....1
   MCCDC, Code C45
   300 Russell Road
   Quantico, Virginia 22134-5130

6. Professor S. Michael, Code EC/Mi.....3
   Department of Electrical and Computer Engineering
   Naval Postgraduate School
   Monterey, California 93943-5121

7. Chairman, Code EC..... 1
   Department of Electrical and Computer Engineering
   Naval Postgraduate School
   Monterey, California 93943-5121

8. Curriculum Officer, Code 34..... 1
   Engineering and Technology
   Naval Postgraduate School
   Monterey, California 93943-5109

9. Professor Ron Pieper, Code EC/Pr..... 1
   Department of Electrical and Computer Engineering

Naval Postgraduate School
Monterey, California 93943-5121

10. Maj Darin McCloy.....1
105 Kinkaid Rd.
Annapolis, Maryland 21402